AD-A098 421 ROCKWELL INTERNATIONAL THOUSAND OAKS CA SCIENCE CENTER F/G 11/2
RESEARCH OF MICROSTRUCTURALLY DEVELOPED TOUGHENING MECHANISMS I--ETC(U)
OCT 80 F F LANGE N00014-77-C-0441
UNCLASSIFIED SC5117.8TR NL

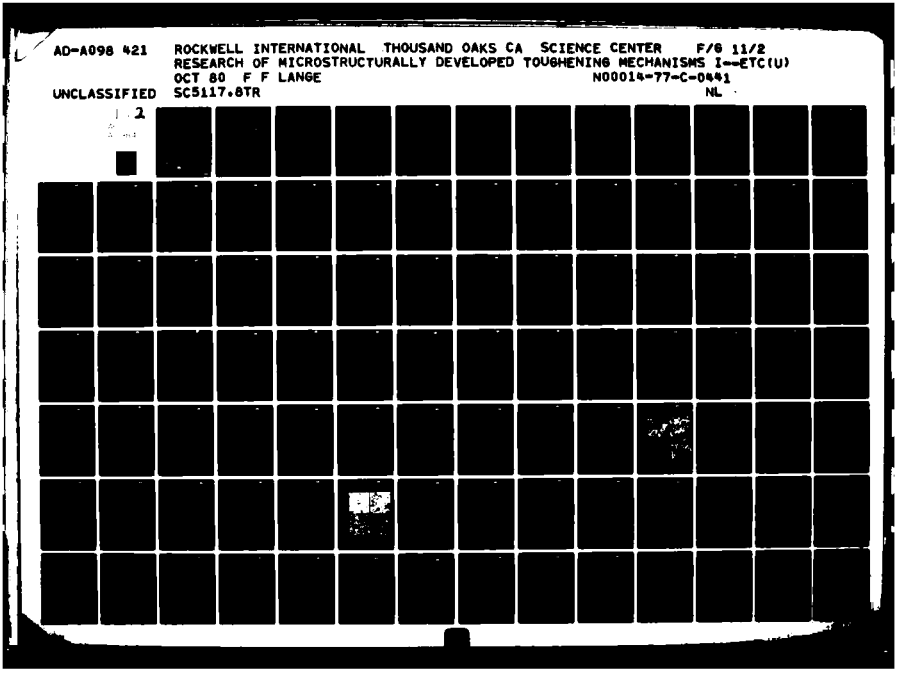

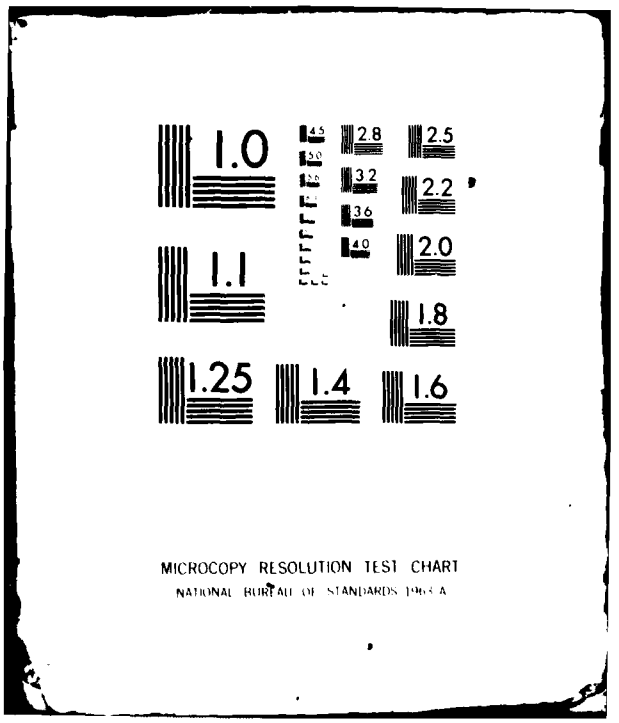
1.0
1.1
1.25
1.4
1.6
1.8
2.0
2.2
2.5
2.8
3.2
3.6
4.0
MICROCOPY RESOLUTION TEST CHART
NATIONAL BUREAU OF STANDARDS 1963 A

LEVEL III

Copy No. 11

RESEARCH OF MICROSTRUCTURALLY DEVELOPED TOUGHENING MECHANISMS IN CERAMICS

TECHNICAL REPORTS NO. 8, 9, 10, 11, 12
FOR PERIOD 12/01/80 THROUGH 04/01/81

CONTRACT NO. N00014-77-C-0441
PROJECT NO. 032-574(471)

PART 1: SIZE EFFECTS ASSOCIATED WITH THE THERMODYNAMICS OF CONSTRAINED TRANSFORMATIONS (SC5117.8TR)

PART 2: CONTRIBUTION TO FRACTURE TOUGHNESS (SC5117.9TR)

PART 3: EXPERIMENTAL OBSERVATIONS IN THE ZrO_2-Y_2O_3 SYSTEM (SC5117.10TR)

PART 4: FABRICATION, FRACTURE TOUGHNESS AND STRENGTH OF Al_2O_3/ZrO_2 COMPOSITE (SC5117.11TR)

PART 5: EFFECT OF TEMPERATURE AND ALLOY ON FRACTURE TOUGHNESS (SC5117.12TR)

AD A098421

DTIC FILE COPY

Prepared for:
Office of Naval Research
Arlington, VA 22217

DTIC ELECTE APR 24 1981 S D A

F. F. Lange

Rockwell International
Science Center

UNCLASSIFIED
SECURITY CLASSIFICATION OF THIS PAGE (When Data Entered)

(9) Technical rept. 1 Dec 80-1 Apr 81

REPORT DOCUMENTATION PAGE

READ INSTRUCTIONS BEFORE COMPLETING FORM

1. REPORT NUMBER
2. GOVT ACCESSION NO. AD-A098421
3. RECIPIENT'S CATALOG NUMBER

4. TITLE (and Subtitle)
(6) Research of Microstructurally Developed Toughening Mechanisms in Ceramics. Parts 1-5.
5. TYPE OF REPORT & PERIOD COVERED
Technical Report No. 8
October, 1980
6. PERFORMING ORG. REPORT NUMBER
(14) SC5117.8TR, SC5117.9TR

7. AUTHOR(s)
(10) F.F. Lange
8. CONTRACT OR GRANT NUMBER(s)
(15) N00014-77-C-0441

9. PERFORMING ORGANIZATION NAME AND ADDRESS
Rockwell International Science Center
1049 Camino dos Rios
Thousand Oaks, CA 91360
10. PROGRAM ELEMENT, PROJECT, TASK AREA & WORK UNIT NUMBERS
032-574(471)

11. CONTROLLING OFFICE NAME AND ADDRESS
(11) Director, Metallurgy Programs, Material Sciences
Office of Naval Research, 800 N. Quincy Street
Arlington, VA 22217
12. REPORT DATE
October 1980
13. NUMBER OF PAGES
27

14. MONITORING AGENCY NAME & ADDRESS (if different from Controlling Office)
(12) 107
15. SECURITY CLASS. (of this report)
Unclassified
15a. DECLASSIFICATION/DOWNGRADING SCHEDULE

16. DISTRIBUTION STATEMENT (of this Report)
Approved for public release; distribution unlimited

17. DISTRIBUTION STATEMENT (of the abstract entered in Block 20, if different from Report)

18. SUPPLEMENTARY NOTES

19. KEY WORDS (Continue on reverse side if necessary and identify by block number)
Fracture toughness, martensitic transformations, ZrO_2, Al_2O_3, phase transformation, strength

20. ABSTRACT (Continue on reverse side if necessary and identify by block number)
The thermodynamics of the constrained phase transformation is presented with particular reference to size effects introduced by surface phenomena concurrent with the transformation, e.g., the formation of solid-solid surfaces (twins, etc.) and solid-vapor surfaces (e.g., microcracks). It is shown that these surface phenomena not only introduce a size dependent energy term into the total free energy change, but also reduce the strain energy associated with the transformation, which can result in a transformation at a temperature where $|\Delta G^c|$ (the chemical free energy change) $< U_{so}$ (the unrelieved

DD FORM 1 JAN 73 1473 EDITION OF 1 NOV 65 IS OBSOLETE

UNCLASSIFIED
SECURITY CLASSIFICATION OF THIS PAGE (When Data Entered)

389949

strain energy associated with the constrained transformation). The results of this analysis lead to a phase diagram representation that includes the size of the transforming inclusion. This diagram can be used to define the critical inclusion size required to prevent the transformation and/or to obtain the transformation, but avoid one or more of the concurrent surface phenomena.

UNCLASSIFIED

SECURITY CLASSIFICATION OF THIS PAGE (When Data Entered)

REPORT DOCUMENTATION PAGE		READ INSTRUCTIONS BEFORE COMPLETING FORM
1. REPORT NUMBER	2. GOVT ACCESSION NO.	3. RECIPIENT'S CATALOG NUMBER
4. TITLE (and Subtitle) Research of Microstructurally Developed Toughening Mechanisms in Ceramics		5. TYPE OF REPORT & PERIOD COVERED Technical Report No. 9 12/01/80 through 04/01/81
		6. PERFORMING ORG. REPORT NUMBER SC5117.9TR
7. AUTHOR(s) F.F. Lange		8. CONTRACT OR GRANT NUMBER(s) N00014-77-C-0441
9. PERFORMING ORGANIZATION NAME AND ADDRESS Rockwell International Science Center 1049 Camino dos Rios Thousand Oaks, CA 91360		10. PROGRAM ELEMENT, PROJECT, TASK AREA & WORK UNIT NUMBERS 032-574(471)
11. CONTROLLING OFFICE NAME AND ADDRESS Director, Metallurgy Programs, Material Sciences Office of Naval Research, 800 N. Quincy Street Arlington, VA 22217		12. REPORT DATE March 1981 13. NUMBER OF PAGES 14
14. MONITORING AGENCY NAME & ADDRESS(if different from Controlling Office)		15. SECURITY CLASS. (of this report) Unclassified 15a. DECLASSIFICATION/DOWNGRADING SCHEDULE

16. DISTRIBUTION STATEMENT (of this Report)

Approved for public release; distribution unlimited

17. DISTRIBUTION STATEMENT (of the abstract entered in Block 20, if different from Report)

18. SUPPLEMENTARY NOTES

19. KEY WORDS (Continue on reverse side if necessary and identify by block number)

Fracture toughness, martensitic transformations, ZrO_2, Al_2O_3, phase transformation, strength

20. ABSTRACT (Continue on reverse side if necessary and identify by block number)

Two approaches are taken to determine the contribution of a stress-induced phase transformation to the fracture toughness of a brittle material. Both approaches result in the expression:

$$K_c = \left[K_o^2 + \frac{2RE_c V_f (|\Delta G^c| - \Delta U_{se} f)}{(1 - \nu_c^2)} \right]^{1/2}$$

DD FORM 1 JAN 73 1473 EDITION OF 1 NOV 65 IS OBSOLETE

UNCLASSIFIED

SECURITY CLASSIFICATION OF THIS PAGE (When Data Entered)

where K_o is the critical stress intensity for the material without the transformation phenomenon, ($|\Delta G^c|$ - U_{sef}) is the work done per unit volume by the stress field to induce the transformation, E_c and ν_c are the elastic properties, V_i is the volume fraction of retained, high temperature phase and R is the size of the transformation zone associated with the crack. It is assumed that only those inclusions (or grains) close to the crack's free surface will contribute to the fracture toughness; thus R $\simeq$ the inclusion size. The chemical free energy change associated with the transformation ($|\Delta G^c|$ will govern the temperature and alloying dependence of the fracture toughness.

UNCLASSIFIED

SECURITY CLASSIFICATION OF THIS PAGE (When Data Entered)

REPORT DOCUMENTATION PAGE		READ INSTRUCTIONS BEFORE COMPLETING FORM
1. REPORT NUMBER	2. GOVT ACCESSION NO.	3. RECIPIENT'S CATALOG NUMBER
4. TITLE (and Subtitle) Research of Microstructurally Developed Toughening Mechanisms in Ceramics		5. TYPE OF REPORT & PERIOD COVERED Technical Report No. 10 12/01/80 through 04/01/81 6. PERFORMING ORG. REPORT NUMBER SC5117.10TR
7. AUTHOR(s) F.F. Lange		8. CONTRACT OR GRANT NUMBER(s) N00014-77-C-0441
9. PERFORMING ORGANIZATION NAME AND ADDRESS Rockwell International Science Center 1049 Camino dos Rios Thousand Oaks, CA 91360		10. PROGRAM ELEMENT, PROJECT, TASK AREA & WORK UNIT NUMBERS 032-574(471)
11. CONTROLLING OFFICE NAME AND ADDRESS Director, Metallurgy Programs, Material Sciences Office of Naval Research, 800 N. Quincy Street Arlington, VA 22217		12. REPORT DATE March 1981 13. NUMBER OF PAGES 19
14. MONITORING AGENCY NAME & ADDRESS(if different from Controlling Office)		15. SECURITY CLASS. (of this report) Unclassified 15a. DECLASSIFICATION/DOWNGRADING SCHEDULE

16. DISTRIBUTION STATEMENT (of this Report)

Approved for public release; distribution unlimited

17. DISTRIBUTION STATEMENT (of the abstract entered in Block 20, if different from Report)

18. SUPPLEMENTARY NOTES

19. KEY WORDS (Continue on reverse side if necessary and identify by block number)

Fracture toughness, martensitic transformations, ZrO_2, Al_2O_3, phase transformation, strength

20. ABSTRACT (Continue on reverse side if necessary and identify by block number)

Materials in the ZrO_2-Y_2O_3 system ($\leq$ 7.5 m/o Y_2O_3) were fabricated to investigate the conditions required to retain the metastable, tetragonal phase and to determine the contribution of the stress-induced martensitic reaction to fracture toughness. Retention of the tetragonal phase was optimized by minimizing porosity and maintaining the grain size below a critical valve. The critical grain size increased from 0.2 μm to 1 μm for compositions ranging between 2 m/o Y_2O_3 to 3 m/o Y_2O_3, respectively. These results are consistent with the theories developed regarding the thermodynamics of the

DD FORM 1 JAN 73 1473 EDITION OF 1 NOV 65 IS OBSOLETE

UNCLASSIFIED

SECURITY CLASSIFICATION OF THIS PAGE (When Data Entered)

martensitic reaction in a constrained state. In the tetragonal plus cubic phase field (compositions between 3.0 and 7.5 m/o Y_2O_3), the critical stress intensity factor decreased from 6.3 MPa·$m^{\frac{1}{2}}$ to 3.0 MPa·$a^{\frac{1}{2}}$ as the volume fraction of the retained, tetragonal phase decreased to zero. Theoretical results, derived from the concept that the crack's stress field does work to unconstrain the transformation, are in good agreement with the experimental results.

UNCLASSIFIED

SECURITY CLASSIFICATION OF THIS PAGE (When Data Entered)

REPORT DOCUMENTATION PAGE		READ INSTRUCTIONS BEFORE COMPLETING FORM
1. REPORT NUMBER	2. GOVT ACCESSION NO.	3. RECIPIENT'S CATALOG NUMBER
4. TITLE (and Subtitle) Research of Microstructurally Developed Toughening Mechanisms in Ceramics		5. TYPE OF REPORT & PERIOD COVERED Technical Report No. 11 12/01/80 through 04/01/81 6. PERFORMING ORG. REPORT NUMBER SC5117.11TR
7. AUTHOR(s) F.F. Lange		8. CONTRACT OR GRANT NUMBER(s) N00014-77-C-0441
9. PERFORMING ORGANIZATION NAME AND ADDRESS Rockwell International Science Center 1049 Camino dos Rios Thousand Oaks, CA 91360		10. PROGRAM ELEMENT, PROJECT, TASK AREA & WORK UNIT NUMBERS 032-574(471)
11. CONTROLLING OFFICE NAME AND ADDRESS Director, Metallurgy Programs, Material Sciences Office of Naval Research, 800 N. Quincy Street Arlington, VA 22217		12. REPORT DATE March 1981 13. NUMBER OF PAGES 21
14. MONITORING AGENCY NAME & ADDRESS(if different from Controlling Office)		15. SECURITY CLASS. (of this report) Unclassified 15a. DECLASSIFICATION/DOWNGRADING SCHEDULE

16. DISTRIBUTION STATEMENT (of this Report)

Approved for public release; distribution unlimited

17. DISTRIBUTION STATEMENT (of the abstract entered in Block 20, if different from Report)

18. SUPPLEMENTARY NOTES

19. KEY WORDS (Continue on reverse side if necessary and identify by block number)

Fracture toughness, martensitic transformations, ZrO_2, Al_2O_3, phase transformation, strength

20. ABSTRACT (Continue on reverse side if necessary and identify by block number)

Three Al_2O_3/ZrO_2 composite series, containing 0, 2 and 7.5 mole % Y_2O_3, were fabricated for fracture toughness determinations. Without Y_2O_3 additions, 2 m/o Y_2O_3 allowed full retention up to 60 v/o ZrO_2. Cubic ZrO_2 was produced with additions of 7.5 m/o Y_2O_3. Significant toughening and strengthening was achieved when tetragonal ZrO_2 was present.

DD FORM 1 JAN 73 1473 EDITION OF 1 NOV 65 IS OBSOLETE

UNCLASSIFIED

SECURITY CLASSIFICATION OF THIS PAGE (When Data Entered)

UNCLASSIFIED

SECURITY CLASSIFICATION OF THIS PAGE (When Data Entered)

REPORT DOCUMENTATION PAGE		READ INSTRUCTIONS BEFORE COMPLETING FORM
1. REPORT NUMBER	2. GOVT ACCESSION NO.	3. RECIPIENT'S CATALOG NUMBER
4. TITLE (and Subtitle) Research of Microstructurally Developed Toughening Mechanisms in Ceramics		5. TYPE OF REPORT & PERIOD COVERED Technical Report No. 12 12/01/80 through 04/01/81
		6. PERFORMING ORG. REPORT NUMBER SC5117.12TR
7. AUTHOR(s) F.F. Lange		8. CONTRACT OR GRANT NUMBER(s) N00014-77-C-0441
9. PERFORMING ORGANIZATION NAME AND ADDRESS Rockwell International Science Center 1049 Camino dos Rios Thousand Oaks, CA 91360		10. PROGRAM ELEMENT, PROJECT, TASK AREA & WORK UNIT NUMBERS 032-574(471)
11. CONTROLLING OFFICE NAME AND ADDRESS Director, Metallurgy Programs, Material Sciences Office of Naval Research, 800 N. Quincy Street Arlington, VA 22217		12. REPORT DATE March 1981 13. NUMBER OF PAGES 21
14. MONITORING AGENCY NAME & ADDRESS(if different from Controlling Office)		15. SECURITY CLASS. (of this report) Unclassified 15a. DECLASSIFICATION/DOWNGRADING SCHEDULE

16. DISTRIBUTION STATEMENT (of this Report)

Approved for public release; distribution unlimited

17. DISTRIBUTION STATEMENT (of the abstract entered in Block 20, if different from Report)

18. SUPPLEMENTARY NOTES

19. KEY WORDS (Continue on reverse side if necessary and identify by block number)

Fracture toughness, martensitic transformations, ZrO_2, Al_2O_3, phase transformation, strength

20. ABSTRACT (Continue on reverse side if necessary and identify by block number)

The critical stress intensity factor (K_c) of materials containing tetragonal ZrO_2 was found to decrease with increasing temperature and CeO_2 alloying additions, as predicted by theory. The temperature dependence of K_c was related to the temperature dependence of the chemical free energy change associated with the tetragonal → monoclinic transformation. Good agreement with thermodynamic data available for pure ZrO_2 was obtained when the size of the transformation zone associated with the crack was equated to the size

DD FORM 1 JAN 73 1473 EDITION OF 1 NOV 65 IS OBSOLETE

UNCLASSIFIED

SECURITY CLASSIFICATION OF THIS PAGE (When Data Entered)

of the ZrO_2 grains. The K_c vs CeO_2 addition data was used to estimate the tetragonal, monoclinic, cubic eutectoid temperature of 270°C in the ZrO_2-CeO_2 binary system.

TRANSFORMATION TOUGHENING

PART 1: SIZE EFFECTS ASSOCIATED WITH THE THERMODYNAMICS OF CONSTRAINED TRANSFORMATIONS

F.F. Lange

Structural Ceramics Group
Rockwell International Science Center
Thousand Oaks, California 91360

Abstract

The thermodynamics of the constrained phase transformation is presented with particular reference to size effects introduced by surface phenomena concurrent with the transformation, e.g., the formation of solid-solid surfaces (twins, etc.) and solid-vapor surfaces (e.g., microcracks). It is shown that these surface phenomena not only introduce a size dependent energy term into the total free energy change, but also reduce the strain energy associated with the transformation, which can result in a transformation at a temperature where $|\Delta G^c|$ (the chemical free energy change) $< U_{se}$ (the unrelieved strain energy associated with the constrained transformation). The results of this analysis lead to a phase diagram representation that includes the size of the transforming inclusion. This diagram can be used to define the critical inclusion size required to prevent the transformation and/or to obtain the transformation, but avoid one or more of the concurrent surface phenomena.

1.0 INTRODUCTION

It has been shown that a stress-induced, phase transformation can be used to increase the fracture toughness of brittle materials based on ZrO_2.[1-5] Metastable, tetragonal ZrO_2 is the toughening agent. Transformation to its stable, monoclinic structure in the vicinity of the crack front is believed to be responsible for the increased fracture toughness. In fabricating these tougher materials, it has been found that retention of the tetragonal structure to room temperature (or below) is critically dependent on the size of the microstructure. Namely, a critical grain size or inclusion size exists, below which the high temperature tetragonal phase can be retained and above which retention is not observed.

Two questions arise from these observations: 1) How can the tetragonal structure be retained upon cooling from its fabrication temperature when it usually undergoes a transformation? 2) How does the stress-induced transformation contribute to fracture toughness? In this part of a series of articles, the theoretical aspects of phase retention will be presented by examining the factors that affect the thermodynamics of a constrained phase transformation. Other articles in this series will address the theory of the toughening phenomena and experimental aspects concerned with phase retention and fracture toughness for materials in the ZrO_2-Y_2O_3 and Al_2O_3-ZrO_2 systems.

2.0 THE $ZrO_2(t) \rightarrow ZrO_2(m)$ TRANSFORMATION

Although the succeeding sections are general for any transformation, the $ZrO_2(t) \rightarrow ZrO_2(m)$ transformation will be used as an example. The tetragonal → monoclinic transformation in this system is athermal, diffusionless and involves both a shear strain and a volume change. The reader is referred to reviews by Subbarao et al[6] and Heuer and Nord[7] for details. Although some differences of opinion exists, Bailey,[8] Bansal and Heuer,[9] and more recently, Buljan et al[10] have shown that the orientation relation between the monoclinic and tetragonal (fcc) unit cells is given by $(110_m) \parallel \{100_t\}$ and $[100_m] \parallel [001_t]$, which can be represented by the "stress-free" or unconstrained strain tensor

$$\tilde{\varepsilon}^t = \begin{pmatrix} \dfrac{a_m \cos\left(\frac{90-\beta}{2}\right) - a_t}{a_t} & 0 & \tan\left(\frac{90-\beta}{2}\right) \\ 0 & \dfrac{b_m - a_t}{a_t} & 0 \\ \tan\left(\frac{90-\beta}{2}\right) & 0 & \dfrac{c_m \cos\left(\frac{90-\beta}{2}\right) - c_t}{c_t} \end{pmatrix} \quad (1)$$

where a, b, c are the cell dimensions of the respective tetragonal (t) and monoclinic (m) structures, and β (<90°) is the monoclinic angle. Substituting the appropriate crystallographic data into Eq. (1), it can be shown that the transformation involves a large shear strain (~ 8%) and a substantial volume increase (3 - 5%).*

*The crystallographic data of Pratil and Subbarao[11] can be extrapolated to room temperature to show that the volume increase changes from 3% at 1150°C to 4.5% at room temperature; β is relatively insensitive to temperature.

During cooling, the tetragonal → monoclinic transformation of pure ZrO_2 begins at ~ 1200°C and proceeds over a temperature range (e.g., 1200° to ~ 600°C) until the transformation is complete.[6] Alloying oxides (e.g., Y_2O_3, CeO_2, etc.) lower the transformation temperature. In this regard, the ZrO_2 - Y_2O_3 system has been best stuided. Srivastaba et al[12] have shown that additions of Y_2O_3 to ZrO_2 lowers the transformation temperature to 565°C where a eutectoid exists at ~ 3.5 m/o Y_2O_3. Scott[13] and Stubican et al[14] appear to be in agreement.

3.0 THERMODYNAMICS OF A CONSTRAINED TRANSFORMATION

Classical theory has shown that retention of the tetragonal structure depends on the magnitude of the strain energy arising from the elastic constraint imposed by surrounding material on shape and volume changes associated with the transformation. Constraint can arise from several sources. First, if the polycrystalline body is single phase, neighboring grains, each with a different crystallographic orientation, will constrain the anisotropic strain of one another. Second, the transforming phase can similarly be constrained by a second phase matrix, as for the case of a two-phase material. The strain energy arising from these constraints can be reduced by microcracking and/or plastic deformation (e.g., twinning). Namely, both microcracking and twinning can accommodate some of the volume and shape change associated with the transformation and can reduce the constraint imposed by the surrounding material. Thus, as will be shown, retention of the tetragonal phase not only depends on the elastic properties of constraining material, but also on the possible occurrence of microcracking and/or twinning during transformation.

3.1 Chemical Free Energy vs Strain Energy

To examine the thermodynamics of the constrained $ZrO_2(t)_2 \rightarrow ZrO_2(m)$ reaction, let us first consider a stress-free, spherical inclusion of the tetragonal phase embedded within a matrix material as shown in Fig. 1a. On transforming to its monoclinic phase,* a state of stress arises within both the transformed inclusion and the surrounding matrix because of the constrained volume and shape change. The differential free energy ($\Delta G_{t\rightarrow m}$) between these two states per unit volume of transformed material is

$$\Delta G_{t\rightarrow m} = G_m^c - G_t^c + U_{se}^m - U_{se}^t + U_S^m - U_S^t$$

or

$$\Delta G_{t\rightarrow m} = -\Delta G^c + \Delta U_{se} + \Delta U_S \quad , \tag{2}$$

where ΔG^c is the chemical free energy (dependent on temperature and composition), ΔU_{se} is the strain energy associated with the transformed particle (for the case considered here $U_{se}^t = 0$ and $\Delta U_{se} = U_{se}^m$) and surrounding matrix which is usually less sensitive to temperature and composition, and ΔU_S is the change in energy associated with the inclusion's surface.

*It is assumed throughout this paper that the whole inclusion transforms in a spontaneous and uniform manner. Although this assumption neglects the conditions for the nucleation and growth usually associated with these transformations, it does allow us to examine the limiting condition concerning the thermodynamic stability of the constrained inclusion.

SC80-9951

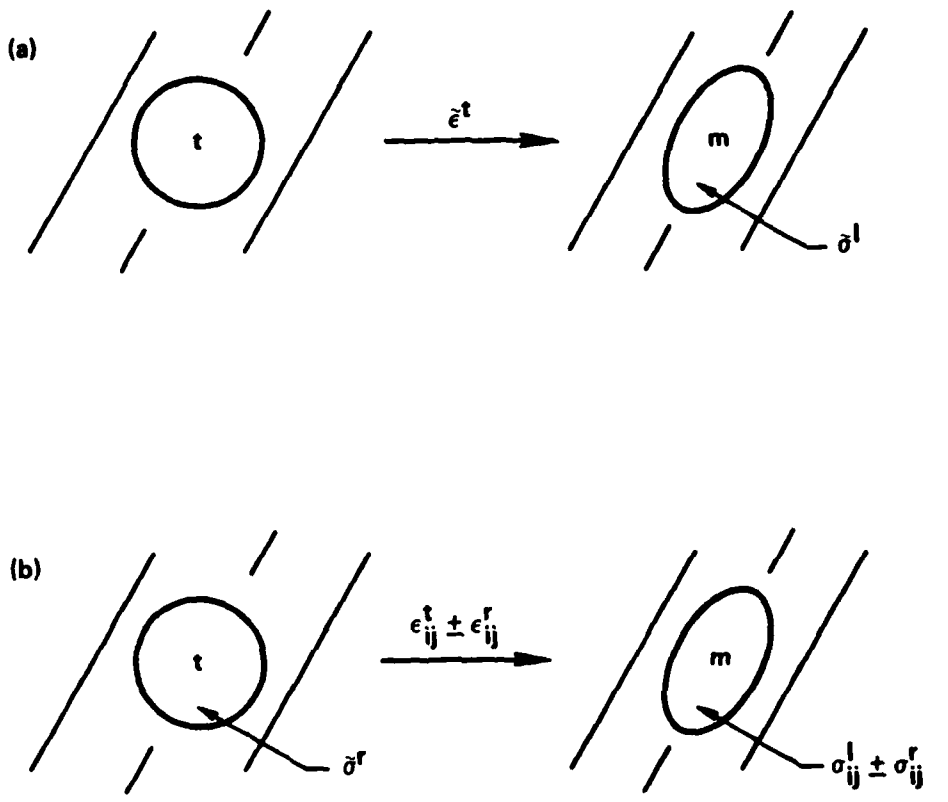

Fig. 1 a) Constrained transformation where initial state (t) is stress free, b) initial state under residual stress ($\tilde{\sigma}_r$).

The condition for the transformation requires that $\Delta G_{t \to m} < 0$, or from Eq. (2)*

$$|\Delta G^c| > U^m_{se} + \Delta U_s \quad . \tag{3}$$

It can be seen that since U^m_{se} is always positive, the constrained transformation temperature will be lower than for the unconstrained case ($|\Delta G^c| > U_s$). That is, constraint lowers the transformation temperature.

The magnitude of the strain energy will depend on the elastic properties of the transformed inclusion and the surrounding matrix, the inclusion shape, and the transformation strain. Eshelby[15] has shown that

$$U^m_{se} = \frac{1}{2} \sigma^I_{ij} \varepsilon^t_{ij} \tag{4}$$

where $\tilde{\sigma}^I$ defines the uniform stress state within the transformed inclusion, and $\tilde{\varepsilon}^t$ is the "stress-free" transformation strain (e.g., given by Eq. (1) for $ZrO_2(t) \rightarrow ZrO_2(m)$).

The effect of the elastic properties of the constraining matrix can be examined by assuming that the transformation only involves an isotropic volume expansion, viz $\varepsilon^t_{ij} = \frac{1}{3} \Delta V/V \, \delta_{ij}$. With this assumption it can be shown that for the case of a sphere

*Throughout this paper, only temperatures where ΔG^c is negative are considered, thus $-\Delta G^c$ is written as $|\Delta G^c|$ for convenience.

$$U_{se}^{m} = \frac{k}{6}\left(\frac{\Delta V}{V}\right)^2 \quad , \tag{5}$$

where

$$k = \frac{2E_1E_2}{(1+\nu_1)E_2 + 2(1-2\nu_2)E_1} \tag{6}$$

and $E_{1,2}$, $\nu_{1,2}$ are Young's modulus and Poisson's ratio of the matrix (1) and transforming particle (2). That is, the greater the elastic modulus of the constraining matrix, the greater the strain energy and, thus, the lower the potential transformation temperature, i.e., the constrained transformation temperature will be inversely proportional to the rigidity of the constraining matrix.*

Alloy additions that lower the unconstrained transformation temperature (i.e., additions such as Y_2O_3 that decrease $|\Delta G^c|$) will also lower the constrained transformation temperature.

3.2 Effect of Residual Stresses

In the preceding section it was assumed that the initial tetragonal state was free of residual stresses. This is not the normal situation since residual stresses will arise during fabrication (e.g., during cooling from the

*It should be pointed out here that the strain energy term in Eq. (2) is only significant for reactions involving relatively small changes in chemical free energy (< several Kcal/mol). It is usually neglected for most chemical reactions where $|\Delta G^c| >> \Delta U_{se}$.

fabrication temperature as a result of thermal expansion mismatch with the matrix phase). As will be shown, these residual stresses will either increase or decrease the strain energy term in Eq. (2) and thus influence the potential transformation temperature.

Figure 1b illustrates the spherical tetragonal inclusion in a state of residual stress and its transformed, monoclinic state. The residual stress state is defined by $\tilde{\sigma}^r$ which, according to Eshelby, arises from a "stress-free" strain $\tilde{\varepsilon}^r$, e.g., the strain an unconstrained inclusion would exhibit due to thermal contraction. The strain energy associated with the tetragonal state is

$$U_{se}^t = \frac{1}{2} \sigma_{ij}^r \varepsilon_{ij}^r \quad . \tag{7}$$

Using the principle of superposition, it can be shown that the strain energy in the transformed, monoclinic state is

$$U_{se}^m = \frac{1}{2} (\sigma_{ij}^I \pm \sigma_{ij}^r)(\varepsilon_{ij}^t \pm \varepsilon_{ij}^r) \quad , \tag{8}$$

where $\tilde{\sigma}^I$ and $\tilde{\varepsilon}^t$ are those stresses and strains defined earlier for the transformation from an unstressed tetragonal particle. The ± sign in front of the residual stress/strain terms in Eq. (8) is to remind the reader that the individual components of these tensors can have either the same sense (+) or the opposite sense (-) relative to the components associated with the transformation.

The free energy change associated with the transformation shown in Fig. 1b is

$$\Delta G_{t\to m} = -\Delta G^{c} + U^{m}_{se} - U^{t}_{se} + \Delta U_{S} \quad . \tag{9}$$

Substituting Eqs. (7) and (8) into (9):

$$\Delta G_{t\to m} = -\Delta G^{c} + U^{o}_{se} \pm \sigma^{I}_{ij}\ \varepsilon^{r}_{ij} \pm \sigma^{r}_{ij}\ \varepsilon^{t}_{ij} + \Delta U_{S} \quad , \tag{10}$$

where U^{o}_{se} is the strain energy defined by Eq. (4) for the case where the tetragonal particle is initially stress free.

Equation (10) illustrates that the residual stress and strain fields either increase or decrease the strain energy depending on their sense. That is, if the transformational fields are compressive and the initial residual fields are tensile, the strain energy is diminished. If, on the other hand, the residual field has the same sense as the transformational field, the strain energy is increased. This latter case will decrease the transformation temperature.

4.0 EFFECT OF INCLUSION SIZE

As mentioned in the Introduction, experiments have shown that the retention of tetragonal ZrO_2 is size dependent. That is, a critical inclusion/grain size exists, below which retention can be achieved and above which it cannot. This size effect cannot be explained by the approach discussed above. What is required is a term in the free energy expression (viz. Eq. 2) which includes the size of the transforming volume.

4.1 Influence of ΔU_S

The change in the surface energy per unit volume (V) of a transformed spherical inclusion can be expressed as

$$\Delta U_S = \frac{A_m\gamma_m - A_t\gamma_t}{V} = \frac{6(\gamma_m - g_s\gamma_t)}{D} \qquad (11)$$

where A_m and A_t are the interfacial surface areas, γ_m and γ_t are the specific interfacial surface energies in the transformed and untransformed states, V (= $\pi/6\ D^3$) is the transformed volume, D is the diameter of the transformed inclusion, and $g_s = A_t/A_m$. Substituting Eq. (7) into Eq. (3) and rearranging, it can be seen that the surface energy term introduces a size effect, i.e., a critical particle size (D_c) above which the energetics of the transformation are statified (viz $\Delta G_{t-m} < 0$) and the transformation can proceed,

$$D > D_c = \frac{6(\gamma_m - g_s\gamma_t)}{[|\Delta G^c| - \Delta U_{se}]} \quad . \qquad (12)$$

Garvie[16] has used a similar argument to explain the experimental observation that unconstrained tetragonal ZrO_2 powders are obtained at room temperature when produced with a particle size < 300A. In order to explain this size effect with the surface energy term, Garvie had to assume that $\gamma_m > g_s\gamma_t^*$. Based on this assumption and the condition that $\Delta U_{se} = 0$ for the case of

*Garvie neglected the possibility of internal surface (twins) in the transformed particles which would have produced the same effect without the assumption that $\gamma_m > \gamma_t$.

unconstrained powders, the critical particle size (D_{uc}) for the powder is

$$D_{uc} = \frac{6(\gamma_m - g_s\gamma_t)}{|\Delta G^c|} \quad . \tag{13}$$

Substituting Eq. (13) into (12) and rearranging, the critical size for the constrained state can be related to the critical size for the unconstrained state by

$$D_c = \frac{D_{uc}}{1 - \frac{\Delta U_{se}}{|\Delta G^c|}} \quad . \tag{14}$$

Examination of Eq. (14) shows that a critical size does exist when $|\Delta G^c| > \Delta U_{se}$ and that $D_c > D_{uc}$.

4.2 Loss of Constraint Through Microcracking and Twinning

As mentioned above, both microcracking and twinning can accompany the $ZrO_2(t) \rightarrow ZrO_2(m)$ transformation. Microcracking and twinning both relieve some of the constraint associated with the volume change and shape change, respectively. In both cases, relief of constraint decreases the strain energy associated with the transformation. As will be shown, the occurrence of microcracking and/or twinning results in a size effect for cases when $|\Delta G^c| < \Delta U_{se}$.

Let us first consider the case of microcracking. Assume that during transformation, a small flaw at the inclusion/matrix interface extends and becomes an arrested microcrack, as shown in Fig. 2a (see Refs. 17, 18 and 19 for the growth requirements of such a crack). A radial crack would be a likely type

SC80-9952

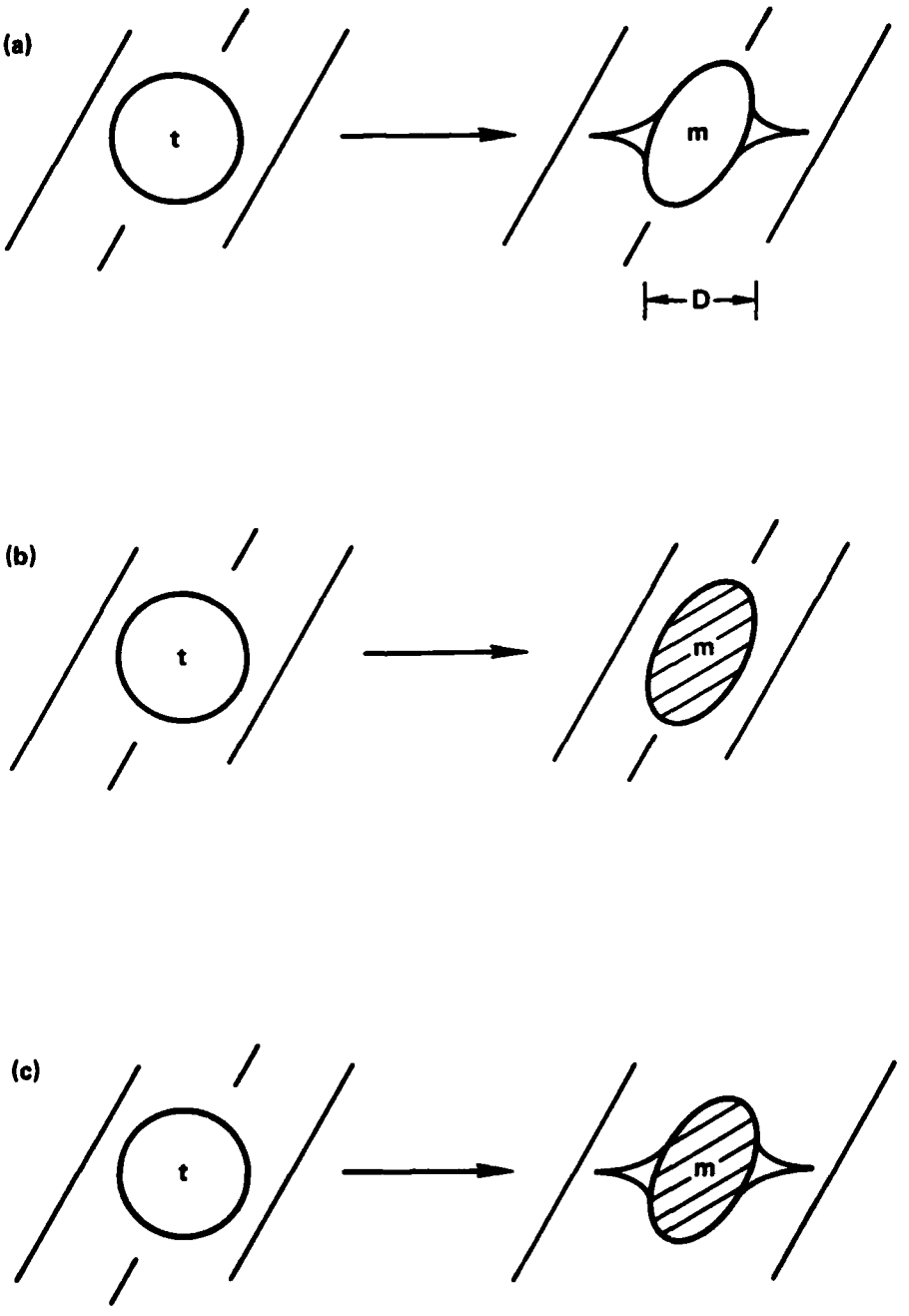

Fig. 2 a) Transformation + microcracking, b) transformation + twinning, c) transformation + microcracking + twinning.

of crack due to the volume expansion associated with the transformed ZrO_2 inclusion. The presence of the crack will change the energetics of the transformed particle in two respects. First, the crack will relieve a fraction $(1 - f_c)$ of the strain energy, ΔU_{se}, associated with the uncracked, transformed system. Second, the crack introduces new surface.

The change in free energy of this microcracked system can be written as follows:

$$\Delta G_{t\to m} = -\Delta G^c + \Delta U_{se} f_c + \frac{A_c \gamma_c}{V} + \Delta U_S \quad . \tag{15}$$

The second from last term in Eq. (15) is the energy per unit volume of transformed material associated with the crack surface; A_c is the area of the crack surfaces, γ_c is the fracture energy per unit area, and V is the volume of the particle. By defining the area of the arrested crack with respect to the inclusion's surface ($A_c = \pi D^2 g_c$) and using $V \simeq 6\pi D^3$, Eq. (15) can be rewritten as

$$\Delta G_{t\to m} = -\Delta G^c + \Delta U_{se} f_c + \frac{6\gamma_c}{D} g_c + \frac{6(\gamma_m - g_s \gamma_t)}{D} \quad . \tag{16}$$

Both f_c and g_c are numerical values that depend on the size of the arrested crack. Previous work[18,19] has shown that f_c and g_c are weak functions of the initial flaw size responsible for the extended microcrack.

Equation (16) shows that the size of the transformed particle is now contained in two terms, i.e., one associated with the energy due to the crack and the other associated with the energy due to the inclusion's surface. Again,

the transformation will only proceed when $\Delta G_{t\to m} < 0$, which from rearranging Eq. (16) defines a critical size for transformation and microcracking.

$$D > D_c^c = \frac{6[\gamma_c g_c + \gamma_m - g_s \gamma_t)}{|\Delta G^c| - \Delta U_{se} f_c} \tag{17}$$

Examination of Eq. (17) shows that the size effect for transformation and microcracking exists when $|\Delta G^c| > \Delta U_{se} f_c$.

Let us now consider the conditions for transformation and twinning (Fig. 2b). In a manner similar to that discussed for microcracking, the energetics of the constrained transformation in which the transformed particle twins can be written as

$$\Delta G_{t\to m} = -\Delta G^c + \Delta U_{se} f_T + \frac{6\gamma_T g_T}{D} + \Delta U_S \quad . \tag{18}$$

The second from the last term is the energy of the twin surface per unit volume of transformed material. Here, the total area of the twin boundaries (A_T) is normalized by the particle's surface area ($g_T = A_T/\pi D^2$). The factors f_T and g_T are dimensionless values, $f_T < 1$, $g_T > 0$; γ_T is the twin boundary energy per unit area.

Similar in all respects to the microcracking phenomena, a critical particle size exists, above which transformation and twinning is possible:

$$D > D_c^T = \frac{6[\gamma_T g_T + \gamma_m - g_c \gamma_t]}{|\Delta G^c| - \Delta U_{se} f_T} \quad . \tag{19}$$

Again, this size effect only exists for the condition $|\Delta G^c| > \Delta U_{se} f_T$.

Now let us consider the case where both microcracking and twinning accompanies the transformation, as shown in Fig. 2c. By using the same approach, it can be shown that a critical inclusion size exists, above which transformation, microcracking and twinning is possible:

$$D > D_c^{c,T} = \frac{6[\gamma_c g_c + \gamma_t g_t + \gamma_m - g_s \gamma_t]}{|\Delta G^c| - \Delta U_{se} f_c f_T} \quad . \tag{20}$$

Likewise, the condition where this size effect will be observed is $|\Delta G^c| > \Delta U_{se} f_c f_T$.

5.0 DISCUSSION

Classical theory of constrained phase transformations, as outlined in the first part of this paper, shows that the potential for lowering the transformation temperature primarily resides with the magnitude of the strain energy that would arise if the transformation were to proceed. For a given transformation, the strain energy depends on the elastic propeties of the constraining matrix and the residual strains that pre-exist in the untransformed state. The strain energy can be maximized by maximizing both the elastic properties of the constraining matrix and the pre-existing residual strains which must have the same sense as the transformational strains. Residual strains of opposite sense decrease the strain energy. For the case of ZrO_2, the ideal constraining matrix would not only have a high elastic modulus, but a higher thermal expansion coefficient than tetragonal ZrO_2.

The constrained transformation temperature can also be decreased by decreasing the change in chemical free energy ($|\Delta G^c|$). This can be accomplished by alloying with an additive (e.g., Y_2O_3, CeO_2, etc.) that is known to decrease the unconstrained transformation temperature.

In addition to these more classical results, it has been shown that the thermodynamics of the constrained transformation depend on the size of the transforming volume. This size effect is introduced through surface changes associated with the transformation. Three different surface related phenomena, viz. microcracking, twinning and microcracking combined with twinning, have the potential for producing a size effect for conditions where $|\Delta G^c| < \Delta U_{se}$. An additional size effect can arise when $|\Delta G^c| > \Delta U_{se}$ due to the changes associated with the inclusion/matrix interfacial energy. The question now is, which of these size effecs is most critical and best explains the experimental observations.

Equations (17), (19), and (20) can be rearranged to express the normalized critical particle sizes for

a) microcracking

$$\frac{D_c^c}{D_{uc}} = \frac{1 + \dfrac{\gamma_c g_c}{(\gamma_m - g_s \gamma_t)}}{1 - \dfrac{\Delta U_{se} f_c}{|\Delta G^c|}} \quad , \tag{21}$$

b) twinning

$$\frac{D_c^T}{D_{uc}} = \frac{1 + \dfrac{\gamma_T g_T}{(\gamma_m - g_c \gamma_t)}}{1 - \dfrac{\Delta U_{se} f_T}{|\Delta G^c|}} \quad , \text{ and} \tag{22}$$

c) microcracking plus twinning

$$\frac{D_c^{c,T}}{D_{uc}} = \frac{1 + \dfrac{\gamma_c g_c + \gamma_T g_T}{(\gamma_m - g_c \gamma_t)}}{1 - \dfrac{\Delta U_{se} f_c f_T}{|\Delta G^c|}} \qquad (23)$$

where D_{uc} is the critical particle size for unconstrained powders as defined by Eq. (13). By making reasonable assumptions concerning the values of f_c, f_T and relative values for the surface energy terms, one can obtain a comparison between Eq. (14), (21), (22) and (23) to judge the dominant size effects.

Recent results of Ito et al.,[19] have shown that a single radial crack in its arrest position relieves ~ 10% of the strain energy associated with the residual stress field of a spherical inclusion. Thus, a value of $f_c = 0.9$ was chosen. Porter[20] has calculated that ~ 70% of the strain energy for the constrained ZrO_2 transformation is associated with the shear strain. Twinning is expected to relieve a large portion, and thus a value of $f_T = 0.67$ was chosen, i.e., it was assumed that 33% can be relieved by twinning. Concerning the surface energy terms, it is reasonable to assume that the cracks' surface energy is greater than both the twin surface energy and the differential interfacial energy of the two states, i.e., $\gamma_c g_c > \gamma_T g_T \approx (\gamma_m - g_s \gamma_t)$. Values chosen are:

$$\frac{\gamma_c g_c}{(\gamma_m - g_s \gamma_t)} = 10$$

and

$$\frac{\gamma_T g_T}{(\gamma_m - g_s \gamma_t)} = 1$$

Substituting the values of these parameters into Eqs. (14), (21), (22) and (23), the normalized particle size was plotted as a function of $\Delta U_{se}/|\Delta G^c|$, as shown in Fig. 3.

Figure 3 maps the size requirements for retaining the tetragonal phase and indicates the type of strain energy relieving phenomena (e.g., twinning, microcracking) that would be observed if these requirements are not met. Since ΔU_{se} is much less dependent on temperature and alloying composition relative to $|\Delta G^c|$, the axis of abscissas in Fig. 3 can either represent increasing temperature or increasing alloy composition.

It should first be noted that the normalized critical size for each phenomena $\rightarrow \infty$ at the temperature where $|\Delta G^c|$ = the relieved strain energy. Also, the rate in which the critical size decreases with temperature is controlled by the numerator of each function. For a given ZrO_2 alloy, the first size effect encountered during cooling (decreasing $\Delta U_{se}/|\Delta G_c|$) will be that due to both microcracking and twinning which, when combined, results in the largest decrease in strain energy. At a given temperature where $|\Delta G^c| > \Delta U_{se} f_c f_T$, transformation will be accompanied by both microcracking and twinning when the normalized size of the transforming inclusion lies above the curve labeled microcracking + twinning. With a further decrease in temperture, i.e., when $|\Delta G^c| > U_{se} f_T$, the size effect for transformation and twinning arises. Normalized particle sizes that fall within the area bounded by the twinning only and microcracking + twinning curves will be transformed and twinned. Figure 3 shows that the condition for transformation and microcracking (at temperatures where $\Delta G^c > \Delta U_{se} f_c$ is only of academic interest. This size requirements is less stringent than the previous two. The last size effect, i.e., due

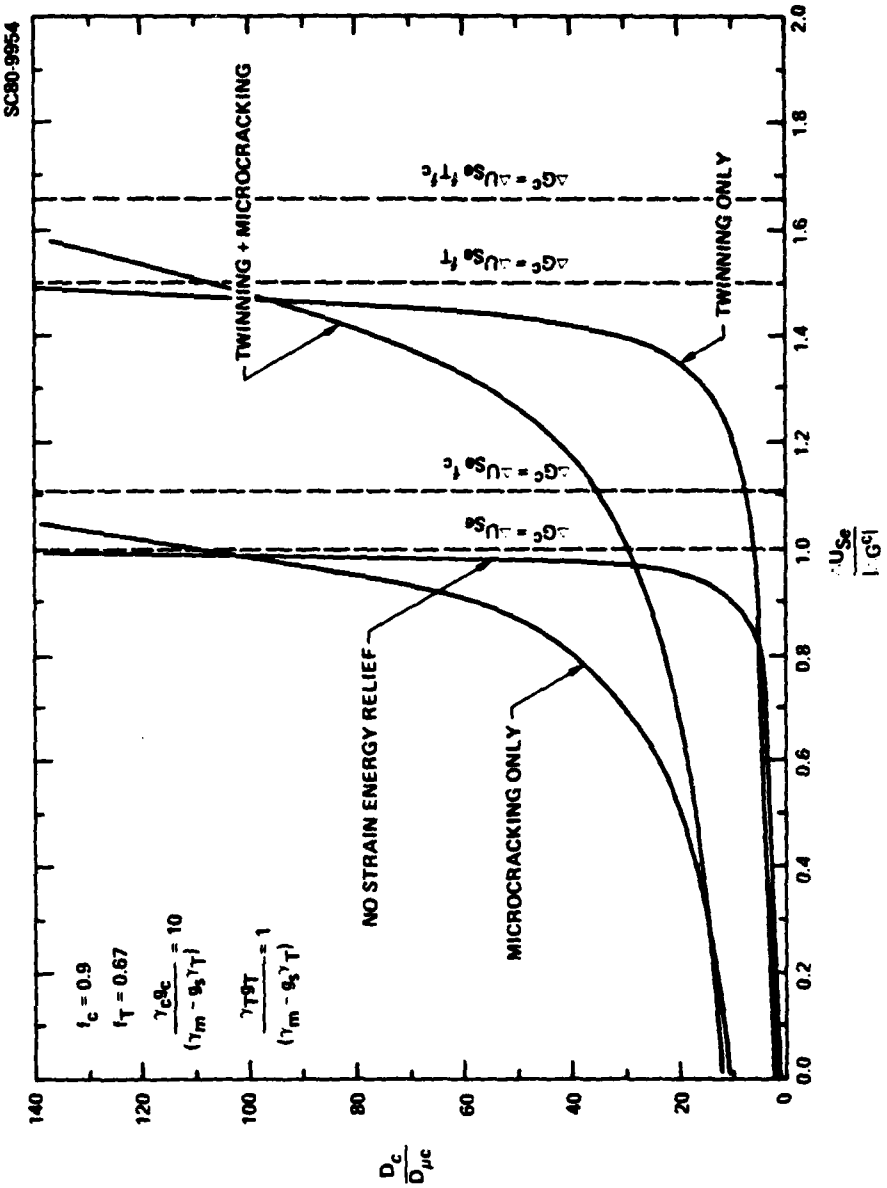

Fig. 3 Plot of conditions where $\Delta G_{tot} = 0$ which includes various surface energy terms as represented in a normalized inclusion (grain) size vs strain energy (ΔU_{se})/chemical free energy (ΔG^c) space.

to the change in interfacial energy, which can only occur at temperatures where $|\Delta G^c| > \Delta U_{se}$, has a limited phase field in Fig. 3 between the curves marked "Twinning Only" (upper bound) and "No Strain Energy Relief" (lower bound). This phase field indicates a limited inclusion size range for transformation without twinning and microcracking.

Since each of the functions illustrated in Fig. 3 defines conditions where $\Delta G_{t\to m} = 0$, it is obvious that these functions define phase boundaries. Therefore, they can be used to construct a phase diagram to indicate the surface phenomena that will or will not accompany a transformation in normalized inclusion size - $\Delta U_{se}/|\Delta G_c|$(e.g., temperature) space. As shown in Fig. 4, four phase fields are evident for the parameters used: 1) a tetragonal field, 2) a monoclinic + twinned + microcracked field, 3) a monoclinic + twinned field, and 4) a monoclinic field without twinning or microcracking. Unlike conventional phase diagrams, Fig. 4 includes the size of the inclusion that is introduced through the various surface energy terms. Although Fig. 4 is derived for specific parameters and would quantitatively change for other parameters, its general character (i.e., phase fields) will remain unchanged if $f_T > f_c$ and $\gamma_c g_c > \gamma_T g_T$.

The phase relations in Fig. 4 predict the following observations. If a composite with a wide distribution of inclusion sizes is cooled to a temperature where $\Delta U_{se}/|\Delta G^c| \simeq 1.2$, there will be a range of inclusions below a critical size still in their tetragonal state. Somewhat larger inclusions will be transformed and twinned, and still larger inclusions will be transformed, twinned and microcracked. If the same composite were only cooled to the

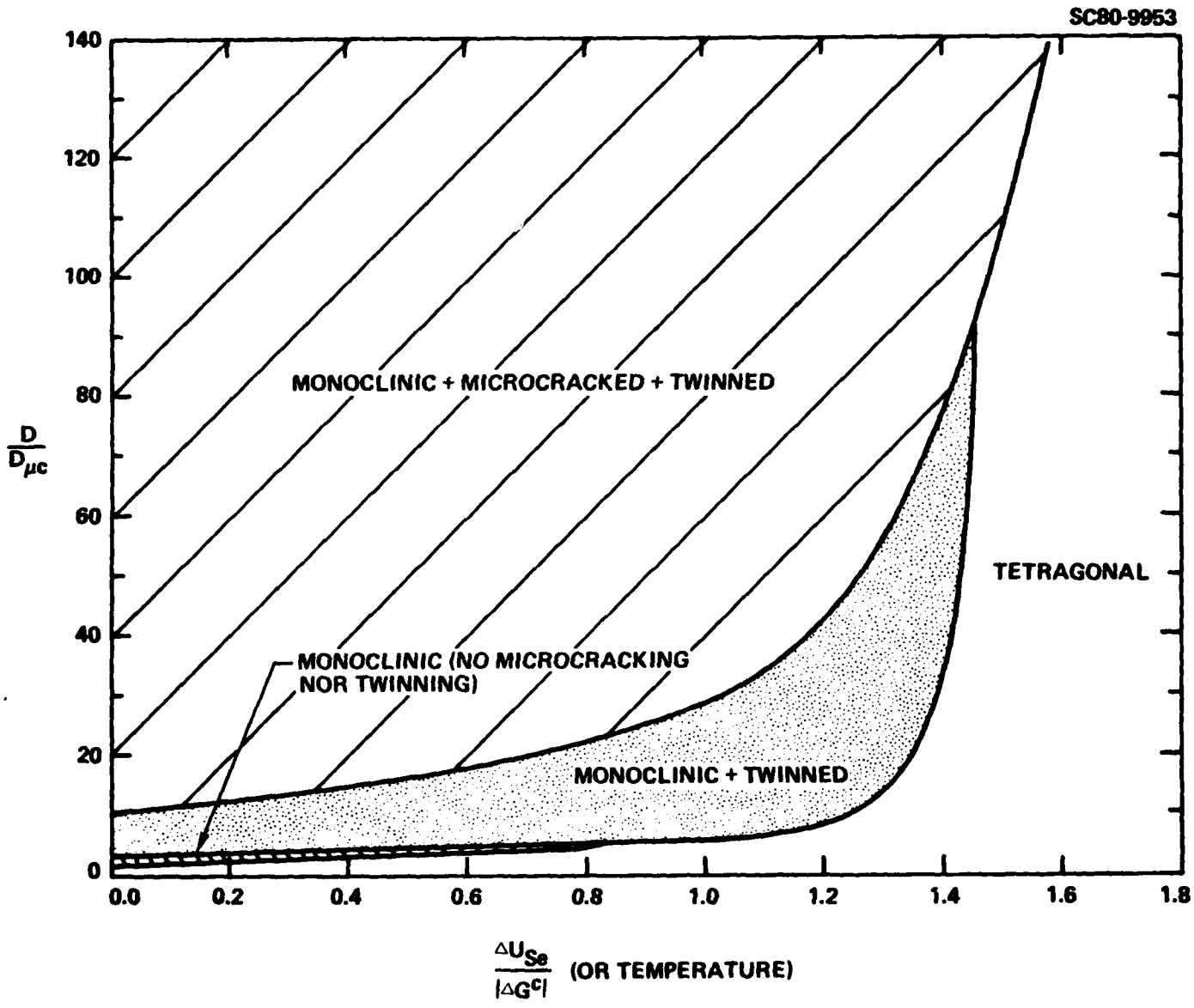

Fig. 4 Phase regions defined by Fig. 3 indicating conditions of transformation and associated surface phenomena as a function of normalized particle size vs temperature of alloy composition.

temperature where $\Delta U_{sc}/|\Delta G^{c}| = 1.55$, inclusions larger than D_c would be transformed, twinned and microcracked; smaller inclusions would be untransformed. Composites with a very narrow size distribution would be in only one of these phase fields. If appropriate experimental techniques were developed to independently observe twinning and microcracking, a composite with a wide inclusion size distribution could be used to experimentally determine the phase boundaries in Fig. 4.

Since the abscissa can also represent increasing alloy composition at a fixed temperature, Fig. 4 can be used to determine the effect of changing alloy composition. For example, at a particular temperature and normalized inclusion size, an increase in alloy content would shift the transformation conditions from one phase field to another; an inclusion-size/composition phase diagram could be constructed at, e.g., room temperature, by heat treating a number of different alloy compositions to increase the inclusion size, and then observing the size required for transformation, twinning and microcracking.

Without specific knowledge of the phase boundaries, it is obvious that the size effects discussed above are critical in fabricating a material in which the object is to retain the high temperature phase upon cooling. If powder routes are used (i.e., sintering), powder sizes $< D_c$ are required since grain growth during sintering is inevitable. If a solid-solution precipitation route is used, heat treatment must be controlled to avoid precipitate growth $> D_c$. Thus, strict microstructural control is required to retain the high temperature phase below its unconstrained transformation temperature.

On the other hand, the objective of fabrication may be to achieve the transformation but to avoid microcracking and/or twinning, as for the case of ferroelectrics. Ferroelectric materials are produced by constrained transformation. Twins (domains) form during the transformation, to primarily relieve strain energy (in non-conducting media, domains also reduce the external electric field due to polarization). Microcracking has also been observed to occur during transformations. The ferroelectric literature sites several grain size phenomena consistent with the agreements leading to Fig. 4. Matsuo and Sasaki[21] showed that when $PbTiO_3$ is fabricated with a grain size ~ 10 μm, a highly microcracked body is produced upon cooling through its transformation temperature; a non-microcracked transformed material could be produced with a grain size of < 3 μm. Buessem et al,[22] indicate that as the grain size of $BaTiO_3$ is reduced to ~ 1 μm, twinning is prevented during the transformation, which leads to a high permittivity. Thus, it can be seen that further work in defining phase fields shown in Fig. 4 are of importance for a variety of useful constrained phase transformations.

ACKNOWLEDGEMENTS

This work was supported by the Office of Naval Research under Contract N00014-77-C-0441. The author deeply appreciated discussions with his colleagues D.J. Green and D.R. Clarke.

REFERENCES

1. R.C. Garvie, R.H. Hannick and R.T. Pascoe, Nature 258, 703 (1975).

2. R.C. Garvie and R.T. Pascoe, Processing of Crystalline Ceramics, ed. by H. Palmour III, R.F. Davis and T.M. Hare, p. 263, Plenum Press (1978).

3. D.L. Porter and A.H. Heuer, J. Am. Ceram. Soc. 60, 183 (1977); ibid. 280 (1977).

4. T.K. Gupta, J.H. Bechtold, R.C.Kuznichi, L.H. adoff and B.R. Rossing, J. Mat. Sci. 12, 2421 (1977).

5. T.K. Gupta, F.F. Lange and J.H. Bechtold, J. Mat. Sci. 13, 1464 (1978).

6. E.C. Sabbarao, H.S. Maiti and K.K. Srivastava, Phys. Stat. Sol. 21, 9 (1974).

7. A. Heuer and G.L. Nord, Jr., Electron Microscopy in Minerology, ed. by H.R. Weuk, p. 274, Springer-Verlag (1976).

8. J.E. Bailey, Proc. Roy. Soc. 279A, 395 (1964).

9. G.K. Bansal and A.H.Heuer, Acta Met. 22, 409 (1974).

10. S.T. Buljan, H.A. McKinstry and V.S. Stubican, J. Am. Ceram. Soc. 59, 351 (1976).

11. R.N. Patil and E.C. Subbarao, J. Appl. Cryst. 2, 281 (1969).

12. K.K. Srivastaba, R.N. Patil, C.B. Chandary, K.V.G.K. Gokhale and E.C. Subbarao, Trans. Brit. Ceram. Soc. 73, 85 (1974).

13. H.G. Scott, J. Mat. Sci. 10, 1527 (1975).

14. V.S. Stubican, R.C. Hink and S.P. Ray, J. Am. Ceram. Soc. 61, 17 (1978).

15. J.D. Eshelby, Progress in Solid Mechanics, Vol. 2, ed. by I.N. Sneddon and R. Hill, p. 89, North-Holland (1961).

16. R.C. Garvie, J. Phys. Chem. 69, 1238 (1965); J. Phys. Chem. 82, 218 (1978).

17. F.F. Lange, Fracture Mechanics of Ceramics, ed. by R.C. Bradt, D.P.H. Hasselman, and F.F. Lange, Vol. 2, p. 599, Plenum Press (1974), ibid Vol. 4 p. 799 (1978).

18. Y.M. Ito, M. Rosenblatt, L.Y. Cheng, F.F. Lange and A.G. Evans, Inter. J. Fracture (in press).

19. Y.M. Ito and F.F. Lange (to be published).

20. D.L. Porter, Ph.D. Thesis, Case-Western University (1977); University Microfilms Int. Order No. 77-25185, 190 pp.

21. Y. Matsuo and H. Sasaki, J. Am. Ceram. Soc. 49, 229 (1966).

22. W.R. Buessem, L.E. Cross and A.K. Goswanii, J. Am. Ceram. Soc. 49, 33 (1966).

Rockwell International
Science Center

SC5117.9TR

TRANSFORMATION TOUGHENING

PART 2: CONTRIBUTION TO FRACTURE TOUGHNESS

F.F. Lange

Structural Ceramics Group
Rockwell International Science Center
Thousand Oaks, California 91360

ABSTRACT

Two approaches are taken to determine the contribution of a stress-induced phase transformation to the fracture toughness of a brittle material. Both approaches result in the expression:

$$K_c = \left[K_o^2 + \frac{2RE_c V_f (|\Delta G^c| - \Delta U_{se} f)}{(1 - \nu_c^2)} \right]^{1/2},$$

where K_o is the critical stress intensity for the material without the transformation phenomenon, $(|\Delta G^c| - U_{se} f)$ is the work done per unit volume by the stress field to induce the transformation, E_c and ν_c are the elastic properties, V_f is the volume fraction of retained, high temperature phase and R is the size of the transformation zone associated with the crack. It is assumed that only those inclusions (or grains) close to the crack's free surface will contribute to the fracture toughness; thus R = the inclusion size. The chemical free energy change associated with the transformation ($|\Delta G^c|$) will govern the temperature and alloying dependence of the fracture toughness.

1. Introduction

The first part[1] of this series described the thermodynamics of the constrained phase transformation with particular emphasis on the effect of the inclusion size. In this part, two different approaches, viz. Griffith's and Irwin's, will be used to determine the contribution of a stress-induced phase transformation to the fracture toughness of a brittle material. As in Part 1, special reference will be made to the ZrO_2 (tetragonal) → ZrO_2 (monoclinic) transformation.

2. Griffith's Approach

In this approach,[2] the total energy of a system, defined as a cracked body and the applied load, is determined as a function of the crack area. The critical condition for crack extension, as first defined by Griffith, corresponds to the maximum in the total energy vs crack area function. To carry out this analysis, we first determine and sum the different contributions to the total energy that change as a function of crack area, viz. the body's strain and surface energies and the load's potential energy. The condition for crack extension is then found by determining the maximum in the total energy vs crack area function. For the needs of the present analysis, we can simplify the analysis by choosing a crack and loading system in which all of the required functions, except the one associated with the stress-induced transformation, are already known. The penny-shaped crack under an applied tensile load first analyzed by Sack[3] was chosen for this analysis.

Figure 1 illustrates a section of the cracked body under tensile load which contains a uniform dispersion of untransformed inclusions of volume fraction V_i. It is assumed that the stress field associated with the crack front has caused inclusions to transform. As the crack extends and the stresses within the previously transformed zone decrease, inclusions that have lost some constraint by being either traversed by the crack or in close proximity to the new fracture surfaces will remain in their transformed state. This process leads to a transformation zone which surrounds the crack, as shown in Fig. 1. Only those inclusions which remain transformed will contribute to the non-recoverable work done by the loading system to stress-induce the transformation. Since the inclusion must lose constraint to remain in their transformed state once the crack's stress field moves, the size of the transformed zone (R) is approximately equal to the inclusion size, viz. $R \simeq D$.

Following Sack's solution to this same problem without the transformation phenomena, the increase in free energy of the body due to new crack surfaces is

$$U_s = \pi c^2 G_0 \quad , \tag{1}$$

where G_0 is the critical strain energy release rate associated with the formation of new surface. The increase in strain energy due to crack extension is

$$U_{se} = \frac{8(1 - \nu_c^2)\sigma_a^2 c^3}{3E_c} \quad , \tag{2}$$

SC81-11763

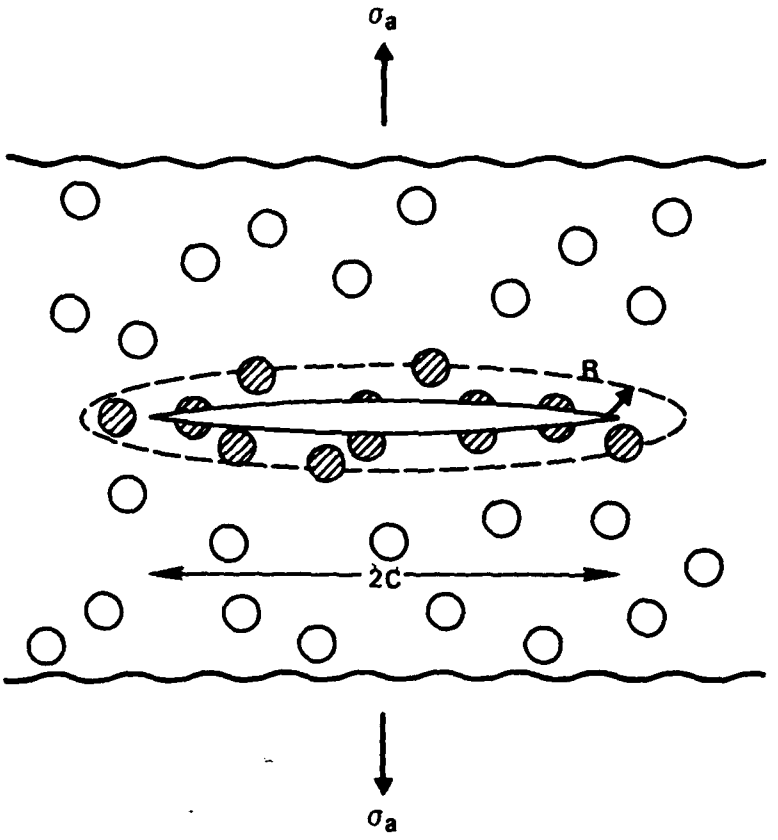

Fig. 1 Section of a penny-shaped crack of radius c within a stressed composite containing inclusions. Hatch inclusions have been transformed during crack extension.

where σ_a is the applied tensile stress and E_c and ν_c are Young's modulus and Poisson's ratio of the composite material, respectively. The work done by the loading system, i.e., the decrease in the potential energy of the load, is

$$W_1 = -\frac{16(1 - \nu_c^2)\,\sigma_a^2 c^3}{3E_c} \quad . \tag{3}$$

An additional term arises when the transformation phenomena is included in the fracture process. Recognizing that the volume of the transformed zone is $2\pi R(c+R)^2 \simeq 2\pi R c^2$, this additional term is the work done by the loading system to form the transformed zone:

$$W_2 = -2\pi R c^2 W V_i \quad ,$$

where W is the work per unit volume of transformed material to induce the transformation. The minimum value of W is determined by

$$\Delta G_{t\to m} = -\Delta G^c + \Delta U_{se} f - W = 0 \quad , \tag{4}$$

where ΔG^c is the chemical free energy change for the reaction ZrO_2 (tetragonal) $\rightarrow$ ZrO_2 (monoclinic), ΔU_{se} is the change in strain energy associated with the transformation and (1 - f) is the loss of strain energy due to the loss of constraint imposed on the inclusions during crack extension. Thus,

$$W = -\Delta G^c + \Delta U_{se} f \tag{5}$$

and*

$$W_2 = 2\pi R c^2 V_f(|\Delta G^c| - \Delta U_{se} f) \tag{6}$$

Summing Eqs. (1), (2), (3), and (6), we obtain the total energy of the system as a function of crack length:

$$U = \pi c^2 G_o + 2\pi R c^2 V_f(|\Delta G^c| - \Delta U_{se} f) - \frac{8(1 - \nu_c^2)\sigma_a^2 c^3}{3E_c} \quad . \tag{7}$$

The condition for crack extension is determined by setting $\delta U/\delta c = 0$, which can be used to define the contribution of the stress-induced transformation to either the strength-crack size relation

$$\sigma_c = \left[\frac{\pi E_c(G_o + 2RV_f(|\Delta G^c| - \Delta U_{se} f))}{4(1 - \nu_c^2)c}\right]^{1/2} \tag{8}$$

or the critical stress intensity factor

$$K_c = \frac{2}{\sqrt{\pi}} \sigma_c \sqrt{c} = \left[K_o^2 + \frac{2RV_f E_c(|\Delta G^c| - \Delta U_{se} f)}{(1 - \nu_c^2)}\right]^{1/2} \tag{9}$$

where $K_o = [(G_o E_c)/(1 - \nu_c^2)]^{1/2}$ is the critical stress intensity factor of the material without the transformation phenomenon.

*The absolute brackets are used to indicate that the sign of ΔG^c has already seen defined as negative in Eq. (4) for the temperature range of interest.

3. Irwin's Approach

The same subject can be viewed with Irwin's approach,[4] where one imposes a force field to a stressed crack tip and calculates the work required to close it by a unit length. Irwin showed that the work per unit length of crack closure is equivalent to the net work dissipated per unit length of crack extension $\partial(U_{se} - W_l)/\partial c$ as calculated through the Griffith approach. Fracture will take place when $\partial(U_{se} - W_l)/\partial c > G_c$, termed the critical strain energy release rate. The major difference between the two approaches is that in calculating the net work dissipated, Irwin only needs to consider the stress field in the vicinity of the crack tip, whereas the Griffith approach requires complete knowledge of the stress state in the system.

To apply the Irwin approach, let us consider the unit of crack to be closed to have traversed a transformed inclusion as shown in Fig. 2(a). The work to close this unit of crack can be broken into two parts, one concerned with the transformation(ΔW_t) and one concerned with crack closure (ΔW_c). The first force field we apply would revert the fractured inclusion back to its untransformed state as shown in Fig. 2(b) The work performed by this first force field per unit volume of transformed material is

$$W = |\Delta G^c| - \Delta U_{se} f \tag{10}$$

where $|\Delta G^c|$ is the change in chemical free energy for reverting the ZrO_2 inclusion from its monoclinic structure to its tetragonal structure. ΔU_{se} is the strain energy associated with the transformation, and (1 - f) is that portion of

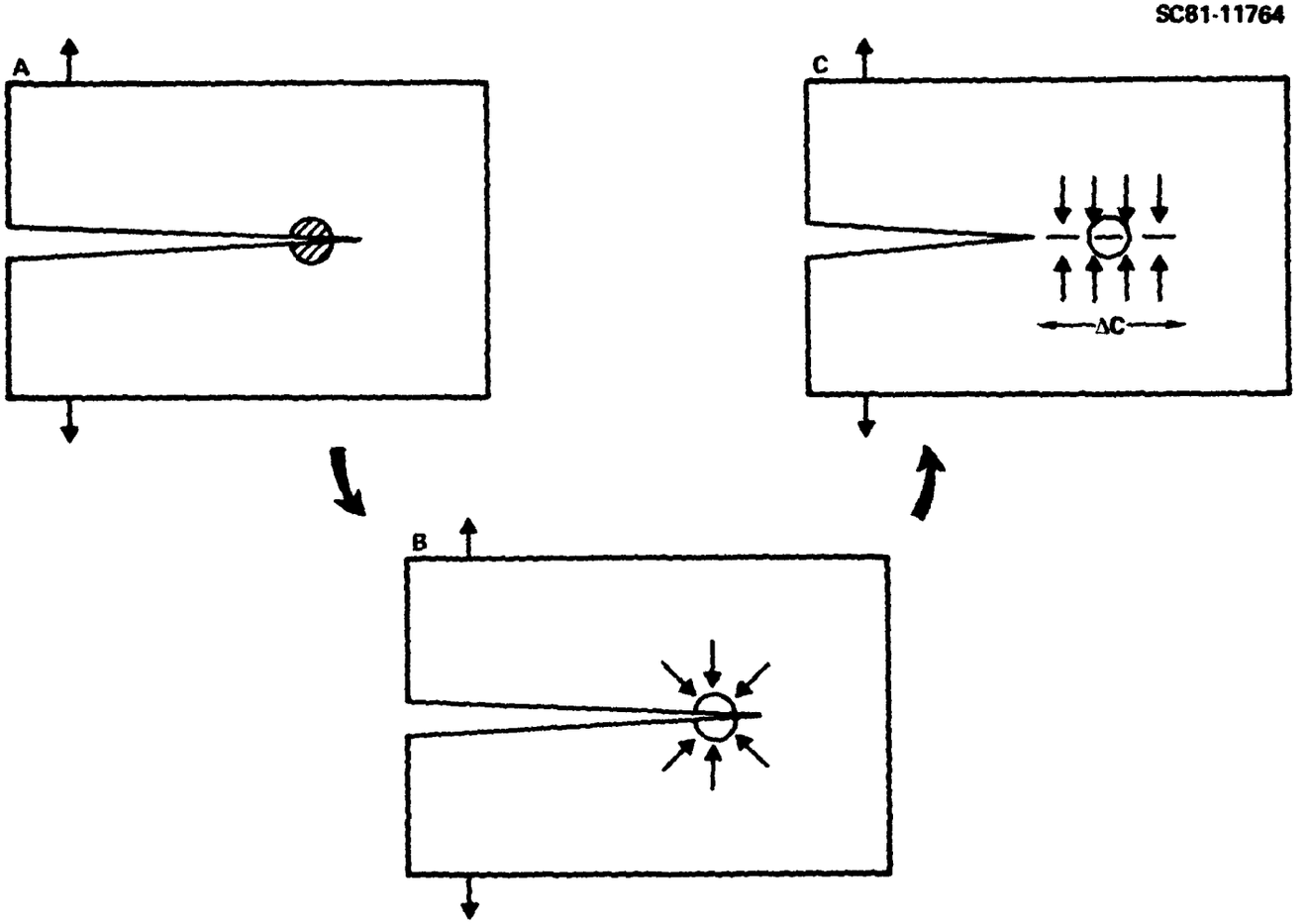

Fig. 2 Crack under fixed grip conditions which has (a) intersected a transformed inclusion (hatched). First force (b) field reverts the inclusion to its untransformed state. Second force field (c) closes crack by a unit length (Δc).

the strain energy relieved during fracture. The total work done on all inclusions within the volume $2R\Delta c$ per unit crack length is

$$\Delta W_t = 2R\Delta c V_i W = 2RV_f(|\Delta G^c| - \Delta U_{se} f)\ \Delta c \tag{11}$$

Once the inclusions have been reverted to their untransformed state, the strain energy associated with the inclusions disappear and the crack now looks like any ordinary crack in a two phase material. At this point, the second force field can be applied, as defined by Irwin, to close the crack by the unit length Δc as shown in Fig. 2(c). The work performed in this operation is

$$\Delta W_c = G_o \Delta c \quad , \tag{12}$$

where G_o is the critical strain energy release rate for the composite material without the transformation phenomenon.

The total work for crack closure per unit crack length which also reverts the inclusions to their initially untransformed state is

$$\frac{\Delta W}{\Delta c} = \frac{\Delta W_c}{\Delta c} + \frac{\Delta W_t}{\Delta c} = G_o + 2RV_f(|\Delta G^c| - \Delta U_{se} f) \quad . \tag{13}$$

Thus, the contribution of the stress-induced transformation to the critical strain energy release rate of the composite can be expressed as

$$G_c = G_o + 2RV_f(|\Delta G^c| - \Delta U_{se} f) \tag{14}$$

or expressed as the critical stress intensity factor

$$K_c = \left[\frac{E_c G_c}{(1 - \nu_c^2)}\right]^{1/2} = \left[K_o^2 + \frac{2RV_f E_c(|\Delta G^c| - \Delta U_{se} f)}{(1 - \nu_c^2)}\right]^{1/2} \tag{15}$$

4. Discussion

As expected, both approaches have led to the same expression for the critical stress intensity factor of a material containing inclusions that can undergo a stress-induced transformation. The expressions show that the contribution of the stress induced transformation can be maximized by maximizing a) the volume fraction (V_f) of inclusions fabricated in their untransformed state, b) the elastic modulus (E_c) of the composite, c) the factor ($|\Delta G^c| - \Delta U_{se} f$) and, d) the size of the transformation zone (R) associated with the propagating crack front. Each of these factors will be discussed in the following paragraphs.

Maximizing the volume fraction would result in a single phase, polycrystalline material, e.g., tetragonal ZrO_2. Here, the inclusions could be defined as individual grains, surrounded by neighboring grains of different misorientations which define the matrix. Each neighboring grain constrains one another from undergoing a stress-free transformation by their anisotropic transformation strains. Thus, from a conceptional viewpoint, a single phase, polycrystalline material can be treated in the same manner as described above.

The elastic modulus of the composite can be increased by choosing a chemically compatible second phase with a higher elastic modulus. For the case of ZrO_2, Al_2O_3, with a modulus approximately twice that of ZrO_2, would be a desirable choice. But adding a second phase to increase the modulus would at the same time decrease the volume fraction (V_i) of the toughening agent. One would, therefore, be concerned with the product of V_iE_c (Eq. (15)) in optimizing K_c. If we assume that the composite modulus is governed by the rule of mixtures, viz. $E_c = E_iV_i + E_m(1 - V_i)$, then the product would have the following form:

$$V_iE_c = V_iE_i[M - V_i(M - 1)] \quad , \tag{16}$$

where $M = E_m/E_i$, the modular ratio of the matrix (m) and the inclusion (i). Differentiating Eq.(16) with respect to V_i,

$$\frac{\partial(V_iE_c)}{\partial V_i} = E_i[M - 2V_i(M - 1)] \quad , \tag{17}$$

shows that the maximum in the product relation occurs at $V_i = 1$ when $M < 2$, i.e., the greatest toughness, with other factors constant, should be obtained for a single phase material. If $M > 2$, the toughness could be optimized when $V_i < 1$. On the other hand, if the objective is to toughen a matrix phase (e.g., toughening Al_2O_3 with ZrO_2), Eq. (16) shows that more toughening is obtained for a given volume fraction the greater the modular ratio. That is, small volume fractions (e.g., $V_i < 0.3$) of the toughening agent will produce greater results the greater the modulus of the matrix material.

The dependence of fracture toughness on temperatures and alloy content will be governed by the factor ($|\Delta G^c| - \Delta U_{se} f$). This is because, relative to other factors, the chemical free energy change(ΔG^c) exhibits the greatest change with temperature and alloying content. For the $ZrO_2(t) \rightarrow ZrO_2(m)$ reaction, $|\Delta G^c|$ decreases with increasing temperature and alloying (e.g., Y_2O_3, CeO_2, etc) content. Thus, for this transformation, the fracture toughness is expected to decrease with increasing temperature as the factor ($|\Delta G^c| - \Delta U_{se} f$) decreases to zero. Likewise, K_c will decrease as the alloy content in $ZrO_2(t)$ is increased. That is, fracture toughness will be optimized at the lower temperatures and for the least alloy content. The temperature where the contribution of the stress-induced toughness disappears will depend on the magnitude of $\Delta U_{se} f$. Phenomena that help relieve strain energy during the fracture, e.g., twinning, will decrease the value of f and thus increase the temperature where the contribution to toughness disappears.

The major assumption used in the model to derive the K_c expressions was that the size of the transformation zone (R) was determined by the close proximity of the inclusions to the free surface formed during fracture. That is, inclusions transformed by the stress field would only remain in their transformed state. once the crack's stress field passes, if much of their constraint was lost during crack extension. This assumption leads to the hypothesis that the zone size would be directly related to the inclusion size (D), viz. $R \approx D$. It is, therefore, hypothesized that K_c will increase with increasing inclusion size.

It can also be argued that if inclusions remote to the crack's surface were to remain in their transformed state, their residual strain energy would be greater relative to those adjacent to the crack surface. Thus, the work loss to the fracture process for remote inclusions would be less than for inclusions adjacent to the crack surfaces. That is, adjacent inclusions would contribute more to the fracture toughness than remote inclusions.

ACKNOWLEDGEMENTS

This work was supported by ONR Contract N00014-77-C-0441.

REFERENCES

1. F.F. Lange, "Part I - Size Effects Associated with Constrained Phase Transformations."

2. A.A. Griffith, "The Phenomena of Rupture and Flow in Solids," Phil. Trans. Roy. Soc., (Lon) 221A, 163 (1920).

3. R.A. Sack, "Extension of Griffiths Theory of Rupture to Three Dimensions," Proc. Phys. Soc. (Lon), 58, 729 (1946).

4. G.R. Irwin, Hanbuck der Physik, Vol. 6, p. 551, Springer, Berlin (1958).

Rockwell International
Science Center

SC5117.10TR

TRANSFORMATION TOUGHENING

PART 3: EXPERIMENTAL OBSERVATIONS IN THE ZrO_2-Y_2O_3 SYSTEM

F.F. Lange

Structural Ceramics Group
Rockwell International Science Center
Thousand Oaks, California 91360

ABSTRACT

Materials in the ZrO_2-Y_2O_3 system (< 7.5 m/o Y_2O_3) were fabricated to investigate the conditions required to retain the metastable, tetragonal phase and to determine the contribution of the stress-induced martensitic reaction to fracture toughness. Retention of the tetragonal phase was optimized by minimizing porosity and maintaining the grain size below a critical valve. The critical grain size increased from 0.2 μm to 1 μm for compositions ranging between 2 m/o Y_2O_3 to 3 m/oY_2O_3, respectively. These results are consistent with the theories developed regarding the thermodynamics of the martensitic reaction in a constrained state. In the tetragonal plus cubic phase field (compositions between 3.0 and 7.5 m/o Y_2O_3), the critical stress intensity factor decreased from 6.3 MPa·$m^{1/2}$ to 3.0 MPa·$m^{1/2}$ as the volume fraction of the retained, tetragonal phase decreased to zero. Theoretical results, derived from the concept that the crack's stress field does work to unconstrain the transformation, are in good agreement with the experimental results.

Introduction

The first part[1] of this series presented a thermodynamic analysis to explain the size effect associated with a constrained phase transformation. It was shown that a critical inclusion (or grain) size exists, below which the constrained transformation is thermodynamically unfavorable. The size effect arises from surface phenomena associated with the transformation, viz. twinning and/or microcracking, which relieve constraint. These surface phenomena can be avoided when the material is fabricated with an inclusion size less than the critical size. It was further shown that the critical size could be increased by either increasing the elastic modulus of the constraining matrix or alloying to lower the chemical free energy change associated with the transformation. From a practical viewpoint, increasing the critical size can relax the constraints imposed on the fabricator who must contend with inclusion coursening and grain growth during heat treatment and/or sintering.

In Part 2,[2] the contribution of the constrained inclusions to the fracture toughness was analyzed. It was shown that the energy absorbed in the fracture process was equivalent to the work performed by the loading system to stress-induce the transformation. The contribution of the stress-induced transformation was thus shown to be related to the chemical free energy change associated with the transformation, the volume of material that remains in the transformed state during crack extension and the elastic modulus of the composite.

The present part reports the experimental work with materials in the ZrO_2-Y_2O_3 system and is concerned with both retention of the high temperature tetragonal structure of ZrO_2 and its effect on fracture toughness. Figure 1 illustrates[3,4] that Y_2O_3 forms a solid solution with ZrO_2 and lowers the tetragonal → monoclinic transformation temperature from ~ 1200°C to ~ 565°C at a Y_2O_3 content of ~ 3.5 mole %. Thus, effects concerned with changing the chemical free energy could be studied with Y_2O_3 additions up to ~ 3.5 m/o. Figure 1 also shows a two phase, tetragonal + cubic, field exists between ~ 3.5 m/o Y_2O_3 and ~ 7 m/o Y_2O_3, in which a two-phase material could be fabricated to determine the effect of the tetragonal phase content on fracure toughness. The ZrO_2-Y_2O_3 system appeared to be useful in obtaining data that may support some of the theoretical predictions made in Parts 1 and 2. In addition, Gupta et al,[5] have already demonstrated that single phase, tetragonal ZrO_2 could be fabricated in this system. Experimental effort was thus concentrated in three areas: 1) effect of density on retention of the tetragonal phase, 2) the critical grain size required for phase retention, and 3) the fracture toughness as related to composition.

3. Experimental Procedures

Composite powders (0 - 7.5 m/o Y_2O_3) were prepared by mixing in a mortar and pestal submicron size ZrO_2 powder* with the appropriate amount of yttrium nitrate in methanol, after determining the conversion factor for the

*Zicar Corp., Florida, N.Y.

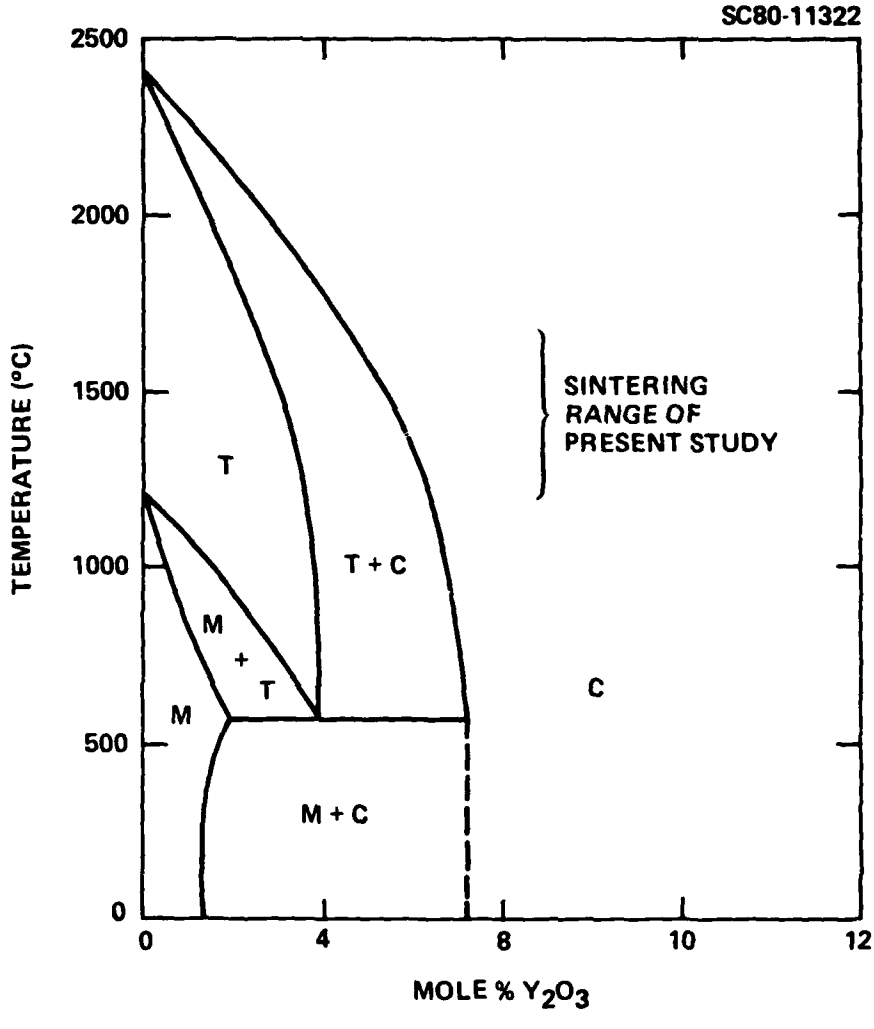

Fig. 1 The portion of the ZrO_2-Y_2O_3 system used in the present work.[3,4]

decomposition of yttrium nitrate to Y_2O_3. Prior to cold pressing and sintering, the composite powders were calcined for 4 hrs at 400°C. Sintering experiments were performed in an air environment at temperatures between 900° and 1650°C. After sintering, densities* were obtained by either dimensional/weight measurements or a water displacement technique. X-ray diffraction was used for phase identification. Monoclinic and tetragonal phase contents were determined from their relative intensity ratios of their respective $(1\bar{1}1)$ and (111) diffraction peaks by using a planometer. The presence of the cubic phase was determined by both the (311) and the (400) diffraction peaks which would split the respective diffraction peaks of the tetragonal phase.

For selected materials the critical stress intensity factor, K_c, was determined at room temperatures by using the indentation technique developed by Evans and Charles.[6] Prior to using this technique, the surface of each specimen was finely polished and x-rayed to ensure that the surface was not noticeably altered by the preparation procedure. It should be noted that rough grinding will induce the tetragonal → monoclinic transformation at the surface, and the damaged layer can be removed (within current detectability limits of ~ 0.5 μm)[7] by polishing. The intercept method was used to determine grain size on SEM micrographs of fracture surfaces.

*The theoretical density of ZrO_2/Y_2O_3 materials were calculated from Scott's[4] lattice parameter data.

3. Results and Discussion

3.1 General Fabrication Observations

Approximately 80% of the total shrinkage occurred rapidly (< 2 hrs) between 1150° and 1250°C; further shrinkage required temperatures > 1350°C. Densities of 82% to 87% theoretical could be achieved at 1200°C/24 hrs. For compositions containing < 6 m/o Y_2O_3, densities of 88% to 93% theoretical could be achieved by sintering 24 hrs at 1200°C followed by 2 hrs at 1400°C. Compositions containing > 6 m/o Y_2O_3 required an additional 2 hrs at 1550°C.

3.2 Retention of Tetragonal ZrO_2: Effect of Density

Composite powders containing 2.5 m/o Y_2O_3 were uniaxial cold pressed at different stresses to achieve different grain densities and then were sintered together for 2 hrs at 1500°C. Figure 2 plots the results of this experiment in terms of the % retained tetragonal phase vs the % of theoretical density achieved during sintering. It can be concluded that the retention of the high temperature tetragonal phase at room temperature depends on the density achieved during fabrication. This conclusion shows that phase retention is directly related to the constraint imposed by neighboring grains on one another. Porosity lowers the elastic modulus and introduces free surface. The effect of both of these factors would reduce the strain energy associated with the transformation allowing larger grains and/or grains bounded by more free surface than neighboring grains to undergo the transformation during cooling.[1]

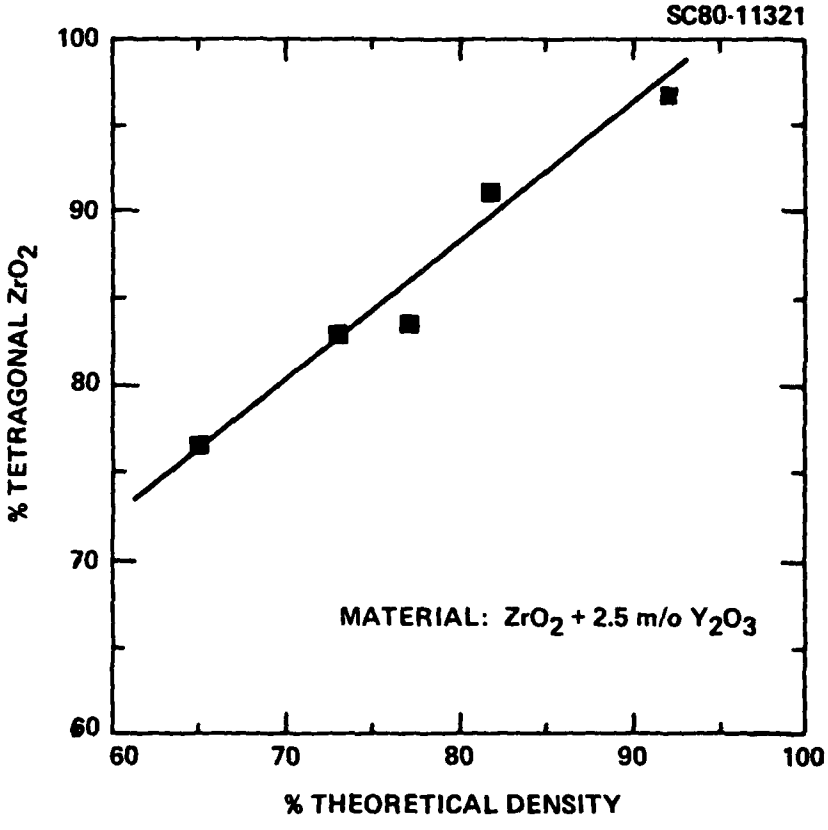

Fig. 2 The effect of density on retention of tetragonal ZrO_2 + 2.5 m/o Y_2O_3.

3.3 Retention of Tetragonal ZrO_2: Critical Grain Size

Composite powders containing 0, 1.5, 2.0, 2.5, 3.0 and 3.5 m/o Y_2O_3 were cold pressed and sintered for 2 hrs at temperatures ranging from 1200° to 1600°C. Detailed grain size measurements were made on the 2.0 m/o Y_2O_3 composition as a function of temperature; these results are shown in Fig. 3. Measurements on other selected compositions were in agreement with these data. The phase content of each specimen was compared to the grain size measurement in order to determine the critical grain size required to retain > 90% of the tetragonal phase. Since densities between 80% and 90% of theoretical could only be achieved with the sintering conditions stated, monoclinic contents < 10% were neglected. (If full density could be achieved, the critical grainsize would be expected[1] to be somewhat smaller than those reported in Fig. 4.)

As shown in Fig. 4, a high tetragonal content could not be achieved for the composition containing 1.5 m/o Y_2O_3, i.e., grain growth during sintering precluded an average grain size < 0.2 μm. The pure ZrO_2 was completely monoclinic under all conditions. More important, Fig. 4 shows that the average critical grain size significantly increases beween 2 and 3 m/o Y_2O_3. The composition containing 3.5 m/o Y_2O_3 contained a detectable amount of cubic phase, indicating that it lies in the tetragonal + cubic phase field at temperatures > 1200°C (see Fig. 1).

The increase in the critical grain size with increasing Y_2O_3 content is consistent with the theortical prediction that the critical grain size would increase as the magnitude of the change in chemical free energy decreases (see Part 1).

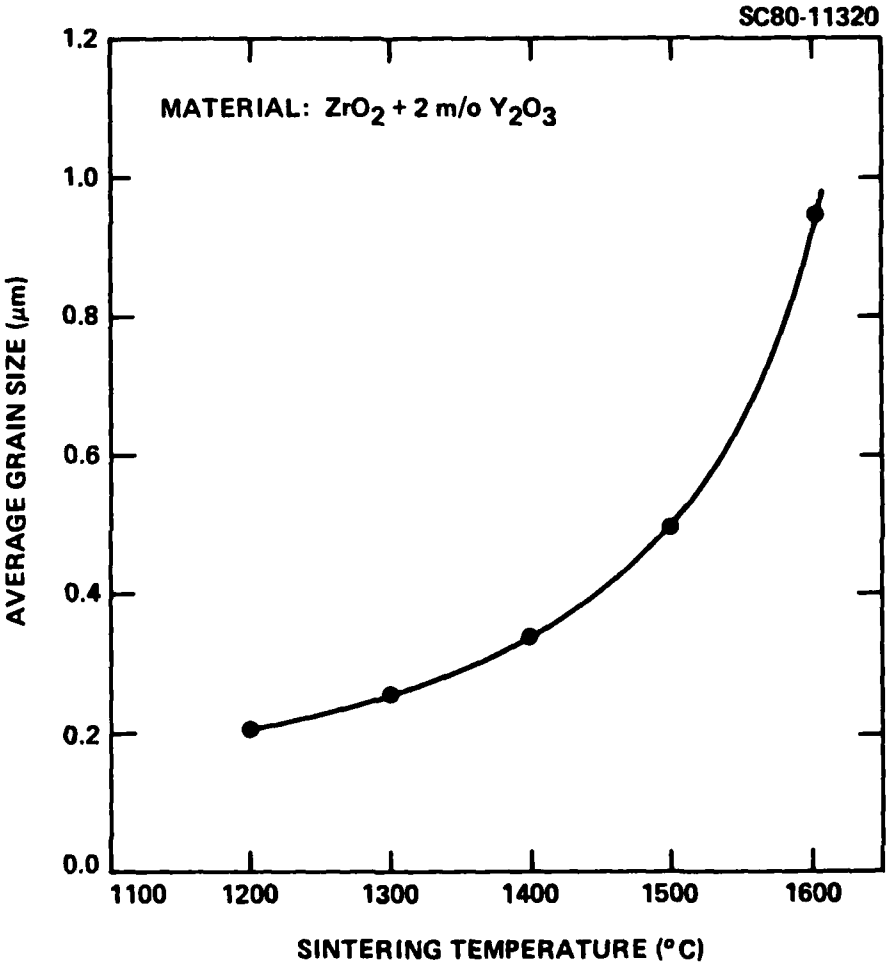

Fig. 3 Average grain size vs sintering temperature determined for the ZrO_2 material containing 2 m/o Y_2O_3.

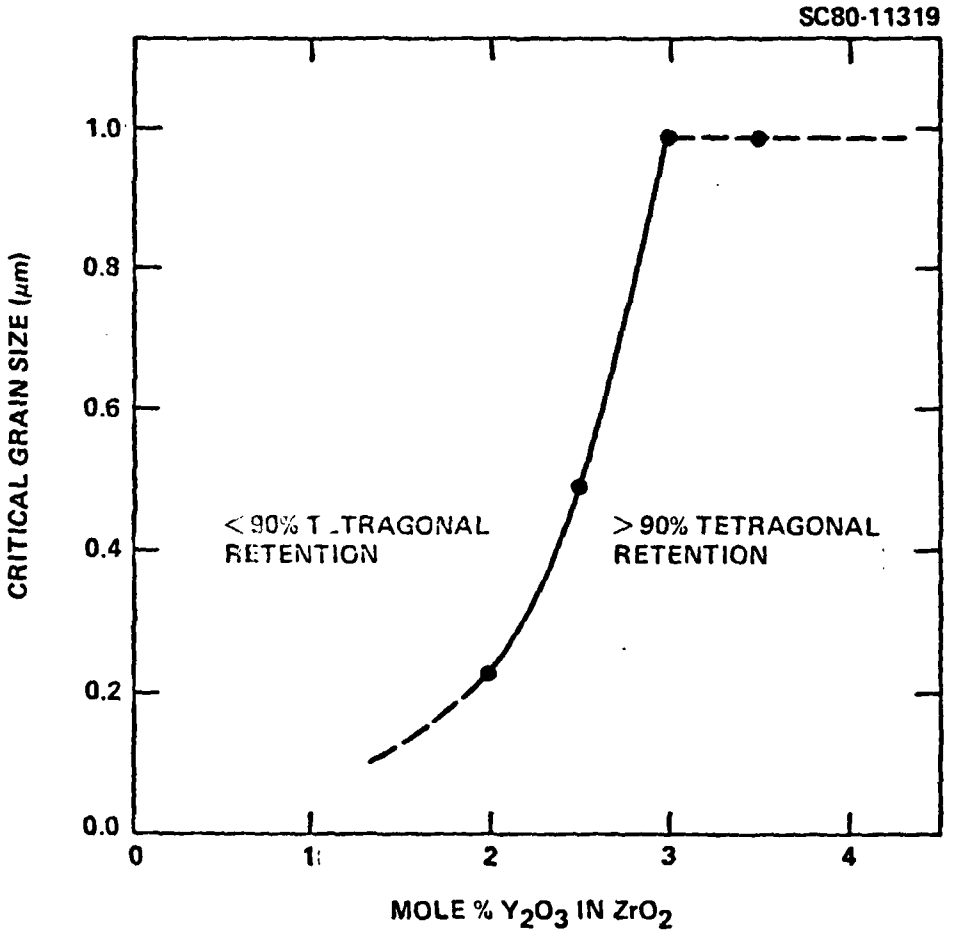

Fig. 4 Critical grain size vs Y_2O_3 content in tetragonal ZrO_2.

3.4 Fracture Toughness

The object of this task was to measure fracture toughness as a function of the retained tetragonal phase. Composite powders containing 1.5 to 7.5 m/o Y_2O_3 in increments of 0.5 m/o Y_2O_3 were prepared. According to Fig. 1, compositions with > 3 m/o Y_2O_3 should contain increasing contents of the cubic phase. Sintering schedules were optimized (see Section 3.1) to produce materials with a density in the range of 88% to 93% of theoretical. Phase identification results were consistent with the concepts required for retention of the tetragonal phase and the phase diagram for this system (Fig. 1). A two phase, tetragonal + cubic, material was produced between 3 m/o Y_2O_3 and 7 m/o Y_2O_3; the volume fraction of the tetragonal phase decreased from one at 3.0 m/o Y_2O_3 to zero at 7.0 m/o Y_2O_3. Only the 1.5 m/o Y_2O_3 composition contained an appreciable amount (> 10%) of the monoclinic phase, because the average grain size was in excess of the critical value. The monoclinic phase was not detected in compositions containing > 3 m/o Y_2O_3.

Results of the stress intensity factor measurements are shown in Fig. 5 as a function of the Y_2O_3 content and the volume content of the tetragonal phase. Three indentations were used to determine K_c for each composition; data scatter illustrates high and low values. This figure shows that K_c drops from 6.3 MPa·$m^{1/2}$ to 3.0 MPa·$m^{1/2}$ as the volume fraction of the tetragonal phase decreases to zero. The 1.5 m/o Y_2O_3 composition had a relatively low K_c due, apparently, to the large amount of monoclinic phase.

The solid line in Fig. 5 was obtained from the calculated effect of the tetragonal volume fraction on K_c by using[2]

SC80-11318

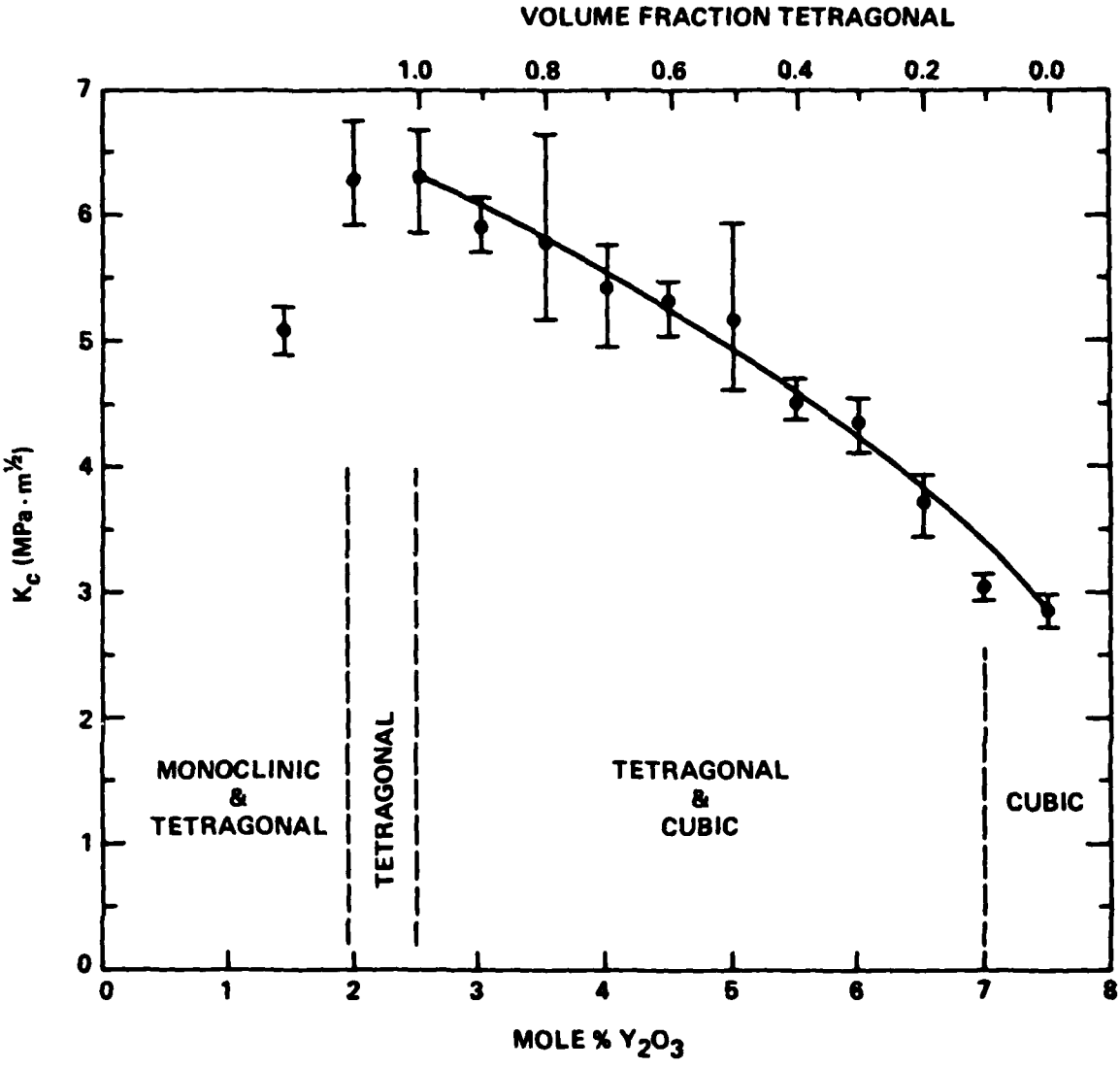

Fig. 5 Fracture toughness (K_c) vs mole % of Y_2O_3 in ZrO_2.

$$K_c = \left[K_o^2 + \frac{2(|\Delta G^c| - \Delta U_{se}f)\, E_c V_i\, R}{(1 - \nu_c^2)} \right]^{1/2} , \qquad (1)$$

where:

K_o = the fracture toughness of the cubic phase (3.0 $MPa \cdot m^{1/2}$),

$|\Delta G^c|$ = the magnitude of the chemical free energy change associated with the transformation,

$\Delta U_{se}f$ = the residual strain energy associated with the transformed grains near the fracture surface

E_c, ν_c = the elastic modulus and Poisson's ratio of the composite,

R = the depth of the transformation zone from the fracture surface, and

V_i = the volume fraction of the tetragonal phase.

Equation (1) can be rewritten as

$$K_c^2 - K_o^2 = C\, V_i , \qquad (2)$$

where C can be evaluated where $V_i = 1.0$ to predict the effect of volume fraction. As shown, the predicted effect of the tetragonal volume fraction on K_c is in perfect agreement with the experimental values.

By assuming that the depth of the transformation zone is approximately equivalent to the grain size,[2] one can use Eq. (1), the experimental values of K_c and K_o, and the expected elastic properties of the material to determine the fac-

tor ($|\Delta G^c|$ - $\Delta U_{se}f$). This factor is the work per unit volume loss during the stress induced transformation.[2] Using the values E_c = 165 GPa*, ν_c = 0.25 and R = 0.5 μm, the work done per unit volume of transformed material was calculated as 176 MJ/m^3.

3.5 Fractography

Figure 6 illustrates the typical fracture surface topography of four compositions (2 m/o Y_2O_3, major: monoclinic, minor: tetragonal; 3.5 m/o Y_2O_3, major: tetragonal, trace: cubic; 7.5 m/o Y_2O_3, major: cubic; 5 m/o Y_2O_3, major: cubic, minor: tetragonal; all ~ 85% dense), sintered at 1600°C for 2 hrs. Intergranular fracture (Fig. 6a) was typical of the high monoclinic materials, suggesting that the crack path followed the intergranular microcracks produced during fabrication as a result of the phase transformation. Such materials were quite friable. Irregular, transgranular fracture was typical of tetragonal materials (Fig. 6b). The irregular fracture topography of individual grains may be a result of the cracks interacting with the complex internal structure of the twinned monoclinic grains. Fig. 6b also indicates that intergranular microcracks were not produced ahead of the crack front, because of the stress-induced transformation, i.e., if microcracks were present, the fracture surface would resemble that shown in Fig. 6a. A smooth transgranular fracture surface was typical for the cubic materials (Fig. 6c). The porosity (~ 15%) associated with these materials is easily recognized in the cubic material because of the near planar topography

*The elastic modulus of dense ZrO_2(t) is 207 GPa,[8] the value of 165 GPa was calculated for a material with 10% porosity.

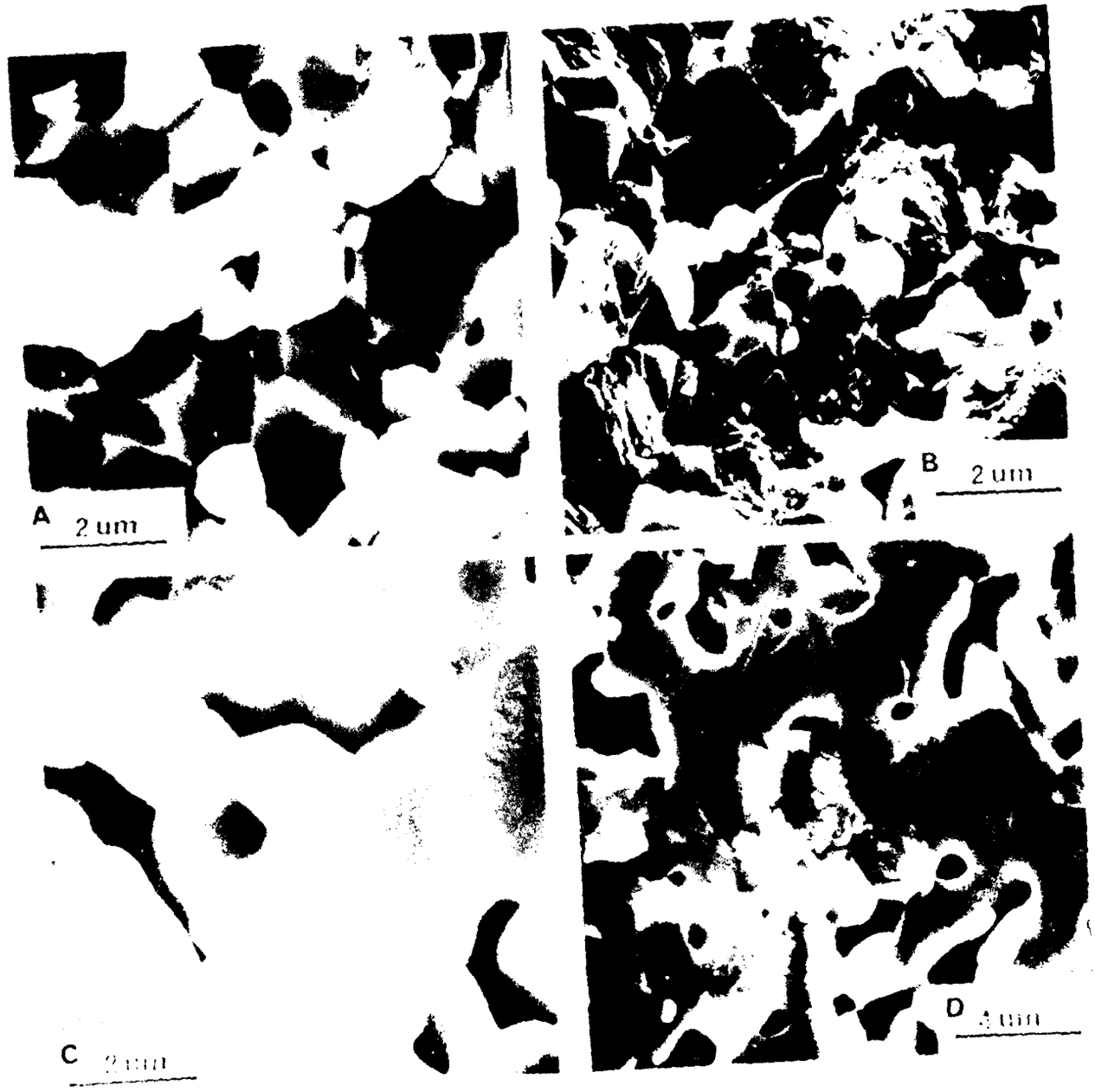

Fig. 6 Fracture surfaces of a) monoclinic ZrO_2 + 2 m/o Y_2O_3 composition, b) tetragonal ZrO_2 + 3.5 m/o Y_2O_3 composition, c) cubic ZrO_2 + 7.5 m/o Y_2O_3, and d) mixed tetragonal + cubic ZrO_2 + 5 m/o Y_2O_3. All sintered at 1600°C/2 hrs.

of the fracture surface. Since both the tetragonal and cubic phases produce different fracture topographies, it was relatively easy to recognize tetragonal grains surrounded by cubic grains for two phase compositions such as the 5 m/o Y_2O_3 composition shown in Fig. 6d. This observation suggests that the two phases in such compositions (3 m/o < Y_2O_3 < 6.5 m/o) are present as separate grains, instead of tetragonal precipitates within a cubic matrix as produced by fabricating in the cubic phase field and quenching into the tetragonal + cubic phase field.[9]

4. Conclusions

Retention of the tetragonal phase was found to depend on both density and grain size. The dependence on density is consistent with the need for self-constraint and with the concepts developed regarding the thermodynamics of the martensitic reaction in an elastically constrained matrix. The effect of Y_2O_3 on the critical grain size is consistent with the theory relating the chemical free energy change to the size effect produced by surface phenomena (e.g., twinning and microcracking) that can accompany the transformation.

The contribution of the stress-induced transformation to the fracture toughness is significant and is directly related to the volume fraction of the retained tetragonal phase. Theory developed to explain this contribution is in good agreement with experimental data validating the concept that the transformation's contribution lies with the work done to unconstrain the martensitic reaction. Fractography indirectly supports this concept.

Acknowledgement

The author wishes to thank M.G. Metcalf for technical services. This work was supported by the Office of Naval Research, Contract N00014-77-C-0441.

References

1. F.F. Lange, "Part 1: Size Effects Associated with Constrained Phase Transformations."

2. F.F. Lange, "Part 2: Contribution to Fracture Toughness."

3. K.K. Srirastaka, R.N. Patil, C.B. Chandry, K.V.G.K. Gokhale and E.C. Subbaro, "Revised Phase Diagram of the System ZrO_2-$YO_{1.5}$," Trans. Brit. Ceram. Soc. 73, 85 (1974).

4. H.G. Scott, "Phase Relations in the Zirconia-Yttria System," J. Mat. Sci, 10, 1527 (1975).

5. T.K. Gupta, F.F. Lange and J.H. Bechtold, "Effect of Stress-Induced Phase Transformation on the Properties of Polycrystalline ZrO_2," J. Mat. Sci 13, 1464 (1978).

6. A.G. Evans and E.A. Charles, "Fracture Toughness Determination by Indentation," J. Am. Ceram. Soc. 59 (7-8), 371 (1976).

7. F.F. Lange and A.G. Evans, "Erosive Damage Depth in Ceramics: A Study on Metastable, Tetragonal Zirconia," J. Am. Ceram. Soc. 62[1], 62 (1979).

8. F.F. Lange, "Part 4: Fabrication, Phase Retention and Fracture Toughness Observations in the Al_2O_3/ZrO_2 System."

9. R.G. Garvie and R.T. Pascoe, Processing in Crystalline Ceramics ed. by H. Palmour III, R.F. Davis and T.M. Hare, p. 263, Plenum Press (1978).

Rockwell International
Science Center

SC5117.11TR

TRANSFORMATION TOUGHENING

PART 4: FABRICATION, FRACTURE TOUGHNESS AND STRENGTH OF Al_2O_3/ZrO_2 COMPOSITES

F.F. Lange

Structural Ceramics Group
Rockwell International Science Center
Thousand Oaks, California 91360

ABSTRACT

Three Al_2O_3/ZrO_2 composite series, containing 0, 2 and 7.5 mole % Y_2O_3, were fabricated for fracture toughness determinations. Without Y_2O_3 additions, tetragonal ZrO_2 could only be retained up to ~ 10 volume % ZrO_2; additions of 2 m/o Y_2O_3 allowed full retention up to 60 v/o ZrO_2. Cubic ZrO_2 was produced with additions of 7.5 m/o Y_2O_3. Significant toughening and strengthening was achieved when tetragonal ZrO_2 was present.

1. Introduction

In Part 1[1] of this series, the thermodynamics of a constrained phase transformation was presented, with particular reference to the size effect associated with retaining the high temperature phase. Part 2[2] presented the theory concerning the contribution of the stress-induced transformation to fracture toughness. Part 3[3] reported experimental observations concerning retention of tetragonal ZrO_2 and its contribution to fracture toughness for a series of materials fabricated in the ZrO_2-Y_2O_3 system. The theory shows that both the critical inclusion size and the contribution to fracture toughness can be increased by chosing a constraining matrix with a higher elastic modulus relative to ZrO_2.

The Al_2O_3-ZrO_2 system was chosen for this study because Al_2O_3 has approximately twice the elastic modulus of ZrO_2 (390 GPa vs 207 GPa) and both phases are chemically compatible with one another.[4] Claussen[5] has already demonstrated that Al_2O_3/ZrO_2 polycrystalline composites could be fabricated, and he also has demonstrated[6] that tetragonal ZrO_2 could be retained in volume fractions up to 0.17. The intent of the present work was to fabricate a series of Al_2O_3/ZrO_2 composite materials from one end-member to the other and to retain the ZrO_2 in its tetragonal state. Initial studies indicated that within the range of fabrication parameters investigated, "pure" tetragonal ZrO_2 could only be retained in volume fractions < 0.10. Based on theoretical considerations (Part 1) and retention studies in the ZrO_2-Y_2O_3 system (Part 3), it was found that additions of 2 m/o Y_2O_3 to the composite powders would allow the retention of the tetragonal phase to much greater volume fractions of ZrO_2. Thus, this series of materials formed the principal base for investigating the contribution of the stress-induced phase transformation to fracture toughness and strength.

2. Experimental

2.1 Fabrication and Phase Identification

Three composite series were fabricated for this study: one containing pure ZrO_2 with volume fractions up to 0.20, one containing ZrO_2 + 2 m/o Y_2O_3* in which tetragonal ZrO_2 was retained, and one containing ZrO_2 + 7.5 m/o Y_2O_3 in which cubic ZrO_2 was obtained. The latter composite series was used for base

*m/o = mole %, v/o = volume %

line information where transformation toughening was not a phenomena associated with the material's fracture mechanics.

Sub-micron powers were used.* Y_2O_3 was introduced as soluble yttrium nitrate.† Composite powders were mixed by ball-milling with methanol and Al_2O_3 balls in a plastic container. All powders were dried; those containing yttrium nitrate were calcined at 400°C for 4 hrs. Densification was achieved by hot-pressing. Most Y_2O_3 containing compositions were hot-pressed at 1600°C/2 hrs; compositions containing 0.8 and 1.0 volume fraction ZrO_2(+2 m/o Y_2O_3) were hot-pressed at 1400°C in order to achieve a smaller grain size which allowed the retention of tetragonal ZrO_2. The non-yttria composites were hot-pressed at 1500°C, again to achieve a smaller grain size for optimizing the retention of tetragonal ZrO_2. The pure Al_2O_3 end-member was hot-pressed at 1400°C to achieve a grain size comparable to the two-phase materials (the introduction of one end-member into the other limited grain growth).

Archimedes' technique was used to measure density of the 5 cm diameter billets. Specimens were cut, ground and polished§ prior to phase identification by x-ray diffraction analysis. Two-theta scans between 27° to 33° were used to estimate the tetragonal/monoclinic ZrO_2 ratio, and scans between 55° to 62° were used to confirm either the tetragonal or the cubic ZrO_2 phase.

---

*Al_2O_3: Lindy B, Union Carbide Corp.; ZrO_2: Zircar Corp.
†Research Chemicals Inc.
§Surface damage caused by cutting and grinding causes the surface to transform. Polishing decreases the depth of the transformed surface layer.

2.2 Mechanical Measurement

Young's modulus (E) of selected compositions was measured at room temperature by the resonance technique with two modes of vibration: flexural (9 kH_3) and extensional (60 kH_3).

The critical stress intensity factor (K_c) was measured on polished specimens by using the indentation technique (20 kgm load) developed by Evans and Charles.[7] Hardness (H) data was also obtained. Three measurements were made for each material.

Flexural strength measurements were obtained in four-point bending (inner span: 1.22 cm, outer span: 2.54 cm) on diamond cut specimens (approximately 0.32 × 0.32 cm cross sectional) finished with a 220 grit diamond grinding wheel.

3. Results

3.1 Fabrication and Phase Identification

Table 1 lists the fabrication conditions for the compositions reported here and their respective average properties. In the series which excluded Y_2O_3, high proportions of tetragonal could only be retained up to ~ 10 v/o ZrO_2. In the series containing 2 m/o Y_2O_3, tetragonal ZrO_2 was fully retained up to ~ 60 v/o ZrO_2. Cubic ZrO_2 was the only ZrO_2 structure observed in the series containing 7.5 m/o Y_2O_3. No 4/Al oxide compounds were observed.

Lattice parameter measurements reported by Scott[8] and confirmed in the present work are a = 5.090Å, c = 5.174Å for the tetragonal (+2 m/o Y_2O_3)

structure and a = 5.135A for the cubic structure. Using these values and the formulation $Zr_{1-x}Y_xO_{2-(x/2)}$, the theoretical densities for the tetragonal and cubic structures were calculated as 6.09 gm/cm^3 and 5.97 gm/cm^3, respectively. Measured densities for the two composite series containing either the tetragonal or the cubic phases obeyed the rule of mixtures for the end-members (Al_2O_3, ρ = 3.98 gm/cm^3), indicating that theoretical density was achieved during fabrication.

Figure 1 illustrates microstructures of the polished surfaces typical of the Al_2O_3/ZrO_2 composites (cracks present were purposely propagated from hardness indents). The observed agglomeration of the minor phase in occasional groups of 2 - 5 grains indicates that the dispersion could be improved. The average ZrO_2 grain size for the composite materials was dependent on the fabrication temperature, viz. ~ 0.2 μm at 1400°C, ~ 0.5 μm at 1500°C and ~ 1 μm at 1600°C. The average grain size for the single phase end members was ~ 2 μm for Al_2O_3 and ~ 0.5 μm for ZrO_2.

As reported in the Appendix, hot-pressed billets containing > 30 v/o Al_2O_3 contained large surface cracks as observed by fluorescent dye penetration. Although small crack-free specimens could be cut and polished for K_c measurements, larger bar specimens invariably contained one or more cracks, which restricted meaningful strength measurements to composites containing < 30 v/o ZrO_2.

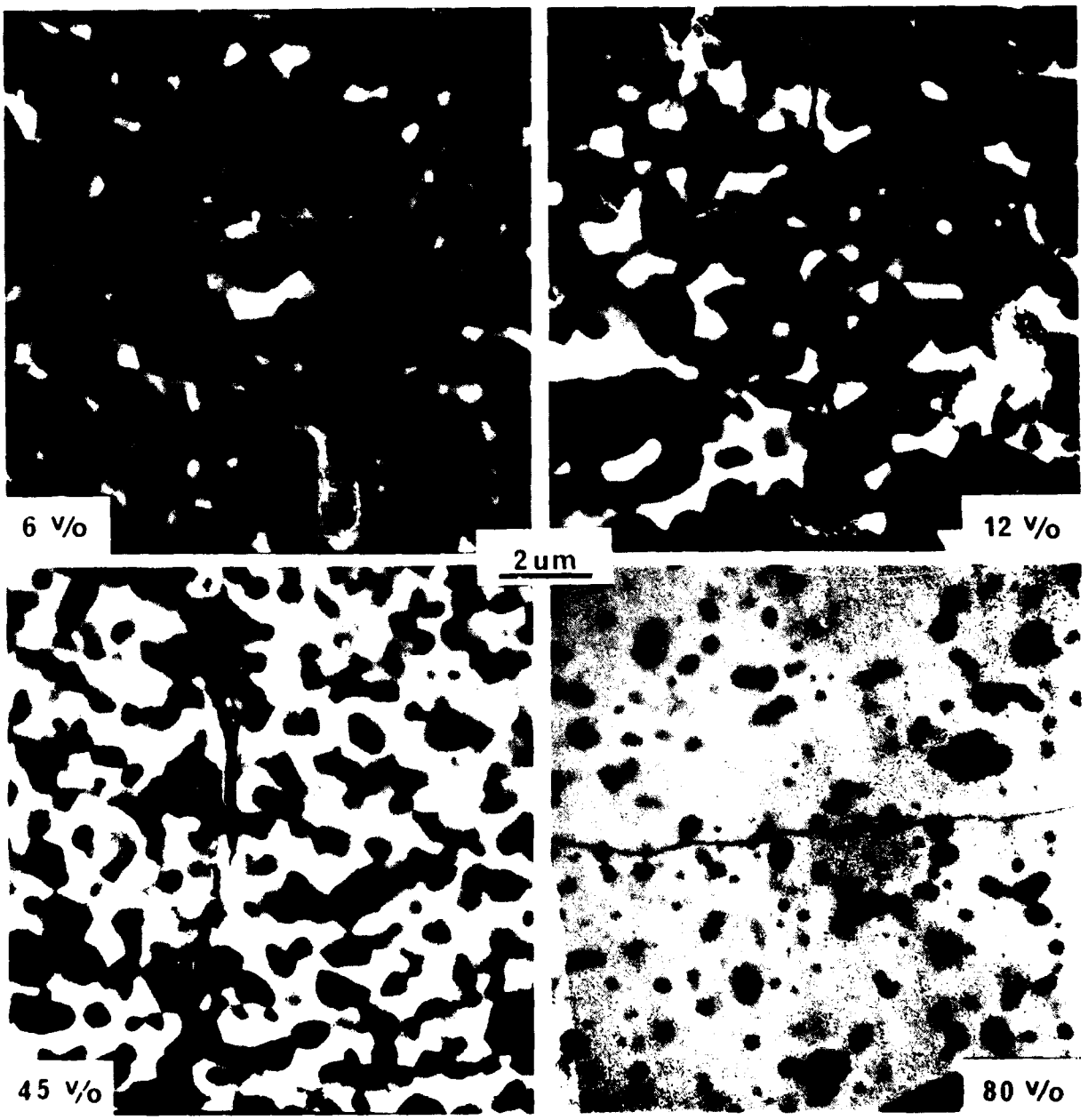

Fig. 1 SEM micrographs of polished surfaces of Al_2O_3/ZrO_2 (+2 m/o Y_2O_3) composites at ZrO_2 volume fractions of 0.063, 0.123, 0.45 and 0.80. Al_2O_3 is dark phase.

3.2 Hardness

Figure 2 illustrates the Vickers hardness (20 kgm) for the Al_2O_3/ZrO_2 (+2 m/o Y_2O_3) series, suggesting that the hardness obeys a linear rule of mixtures. The 20 v/o ZrO_2 (pure) composition had an exceptionally low hardness (see Table 1). Its high monoclinic content and friable nature suggested that it contained a high density of microcracks. SEM observations adjacent to the hardness indent in this material indicated that the indenter pushed the microcracked material aside as it extended into the interior.

3.3 Young's Modulus

Figure 3 reports the Young's modulus of the Al_2O_3/ZrO_2 (+2 m/o Y_2O_3) series obtained from the two resonance techniques.

3.4 Critical Stress Intensity Factor

Figure 4a reports K_c as a function of composition for the two series containing Y_2O_3. A considerable increase in fracture toughness could be achieved with the addition of the tetragonal ZrO_2 (viz. the 2 m/o Y_2O_3 series). In contrast, the addition of cubic ZrO_2 lowered the fracture toughness (viz. the 7.5 m/o Y_2O_3 series). Figure 4b shows that the peak in K_c for the series that excluded Y_2O_3 corresponds to the maximum retention of the tetragonal phase in this series.

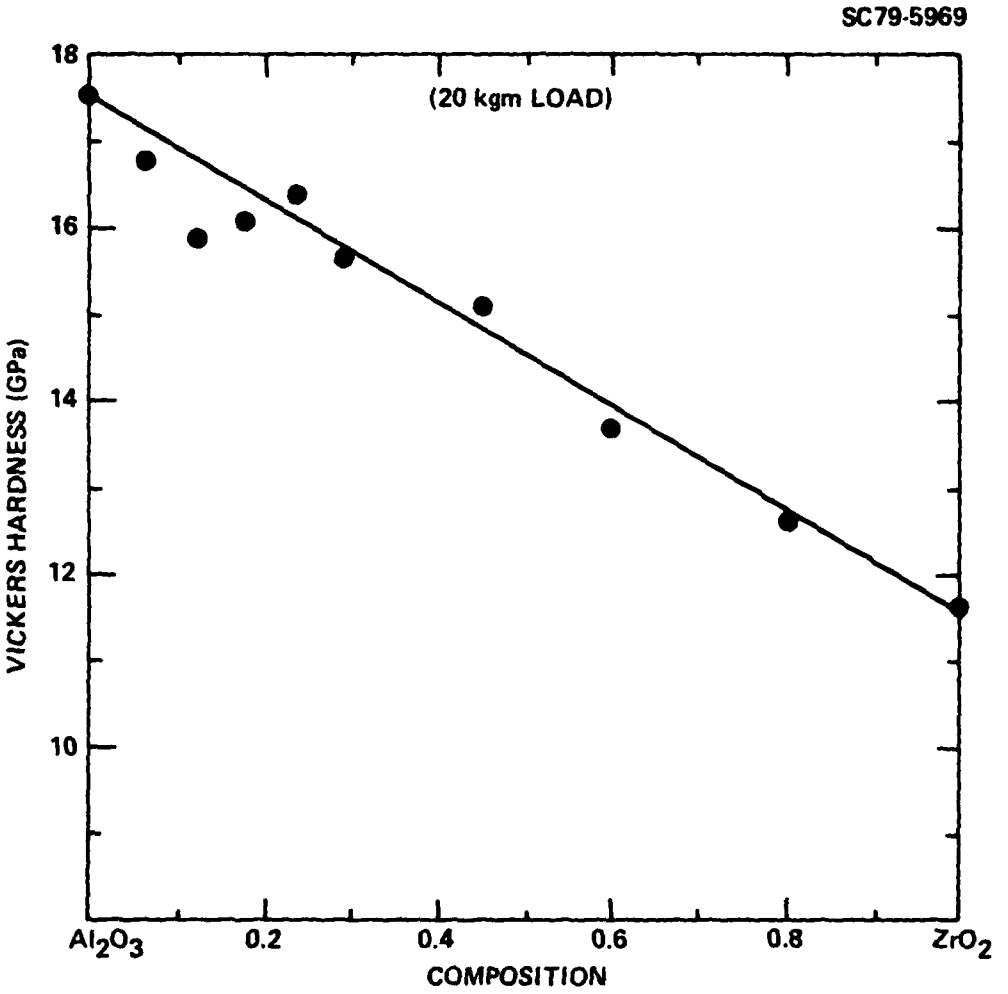

Fig. 2 Vicker's hardness (measured at 20 kgm) for the Al_2O_3/ZrO_2 (+2 m/o Y_2O_3) composite series.

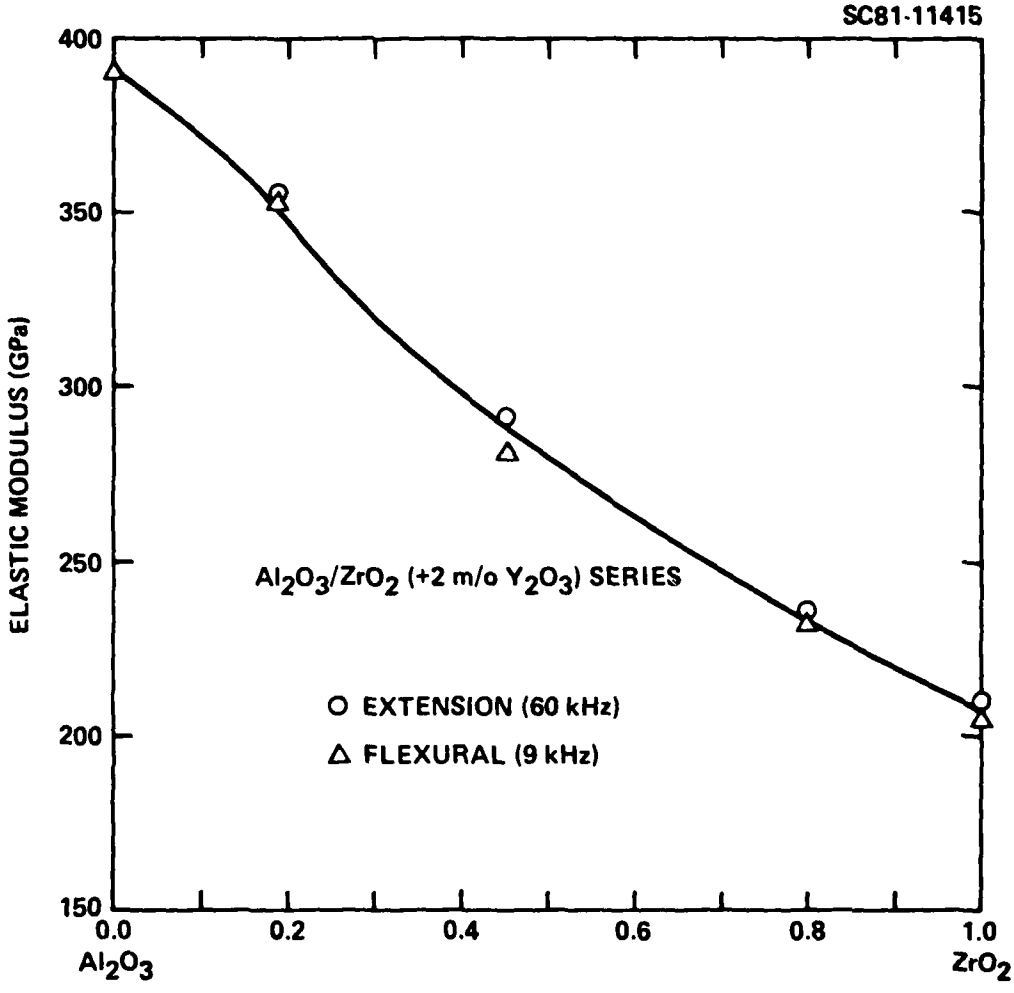

Fig. 3 Young's modulus vs composition for the Al_2O_3/ZrO_2 (+2 m/o Y_2O_3) series.

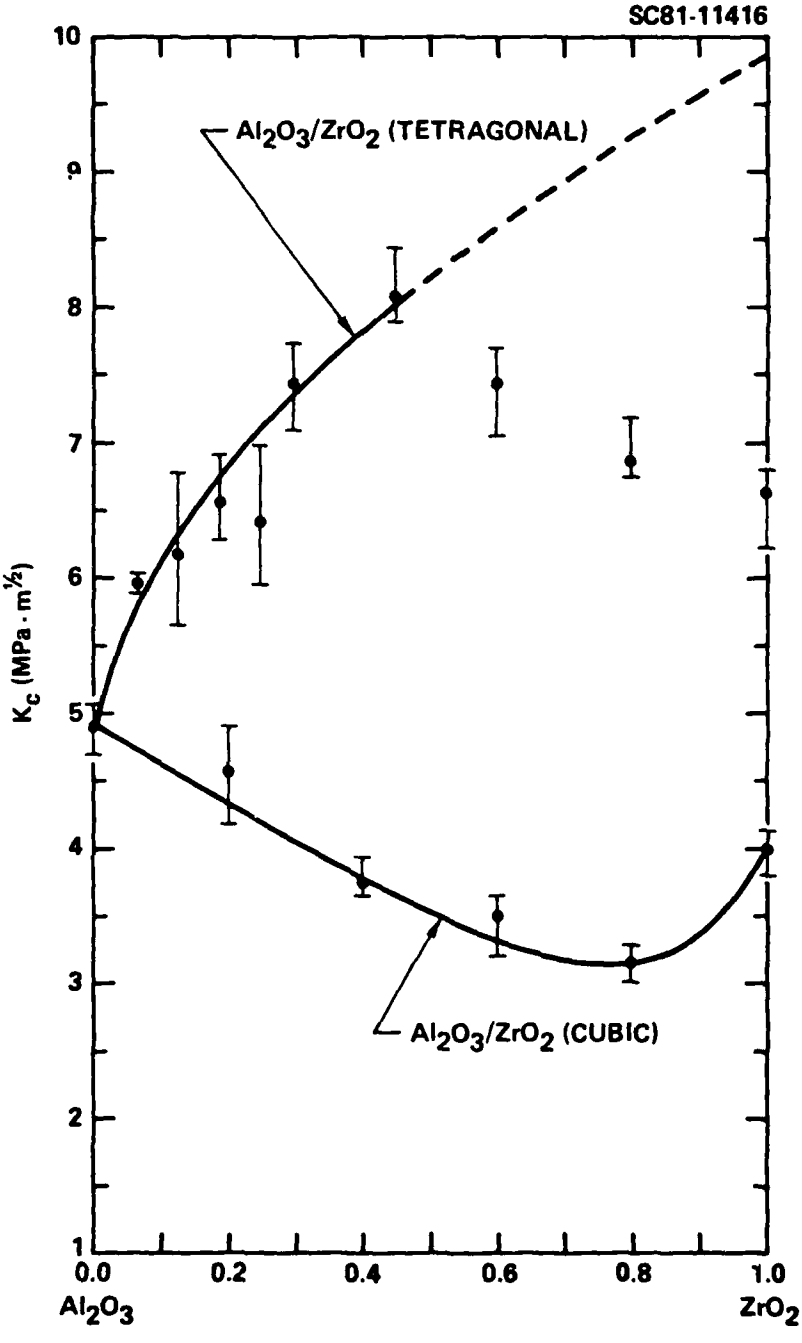

Fig. 4 a) Critical stress intensity factor vs composition for the Al_2O_3/ZrO_2 (+2 m/o Y_2O_3) (circles) and the Al_2O_3/ZrO_2 (+7.5 m/o Y_2O_3) series (squares).

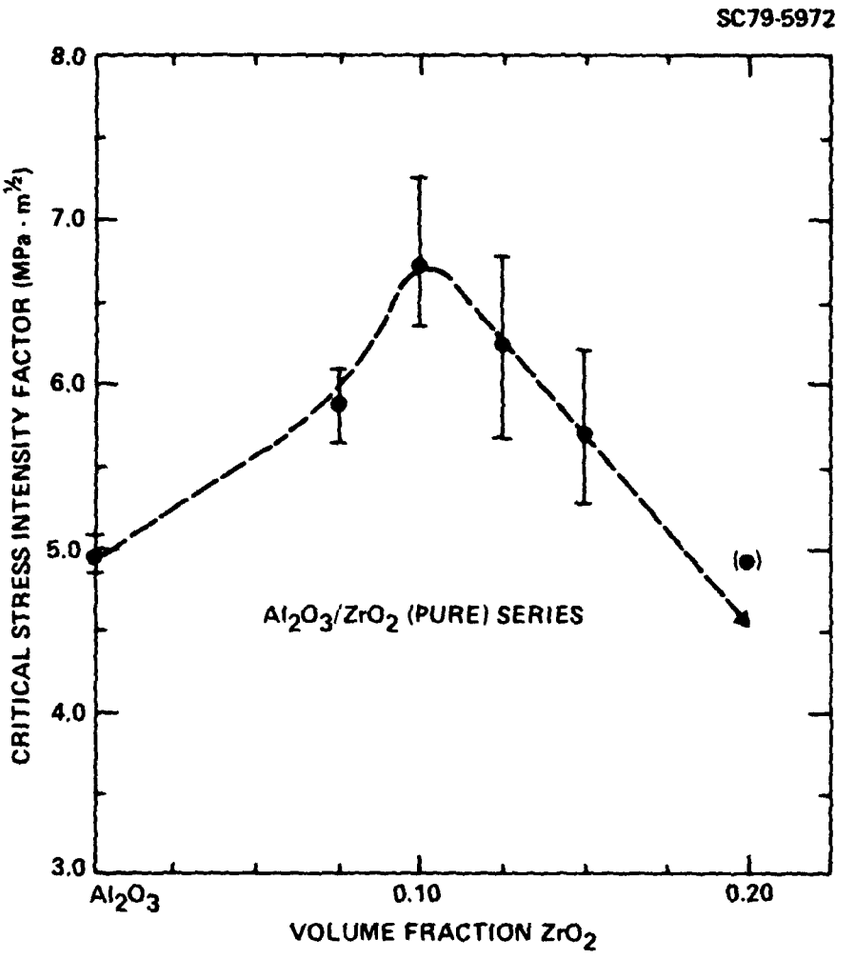

Fig. 4 b) Critical stress intensity factor vs composition for the Al_2O_3/ZrO_2 (pure) series.

3.5 Strength

Flexural strength determinations for the series containing 2 m/o Y_2O_3 are shown in Fig. 5. Since it is known that surface grinding can result in compressive surface stresses in these types of meterials, a set of specimens were annealed at 1300°C prior to testing to eliminate the transformed surface layer. Annealing resulted in a lower average strength. It is interesting to note that significant strengthening of Al_2O_3 can be achieved by adding the tetragonal ZrO_2 toughening agent.

4. Discussion

4.1 Retention of Tetragonal ZrO_2

Part 1 of this series showed that the critical grain size for retaining the high temperature, tetragonal structure of ZrO_2 could be increased by increasing the elastic modulus of the constraining matrix and by alloying to decrease the chemical free energy change. Data presented here are consistent with these theoretical conclusions. Namely, without Y_2O_3 additions, retention of tetragonal ZrO_2 became more difficult as the elastic modulus of the composite decreased. Additions of 2 m/o Y_2O_3 resulted in phase retention to much large ZrO_2 volume fractions, despite the decreased modulus and larger grain size. Part 3 of this series showed that the critical grain size for ZrO_2 (+2 m/o Y_2O_3) was ~ 0.2 μm when the constraining matrix was ZrO_2. The current study shows that the critical grain size can be increased to at least 1 μm with the higher modulus of the Al_2O_3/ZrO_2 constraining matrix. Also note that as the composition approached the ZrO_2 end-member, the fraction of retained tetragonal phase decreased.

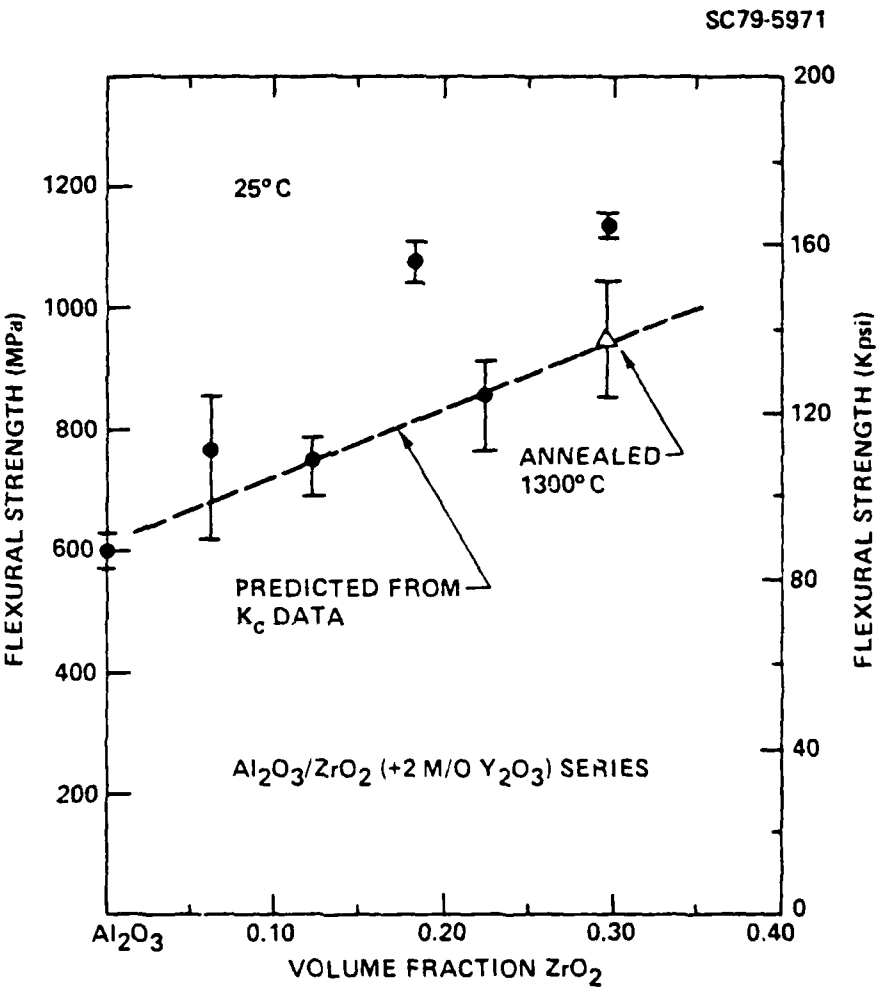

Fig. 5 Flexural strength vs composition for the Al_2O_3/ZrO_2 (+2 m/o Y_2O_3) series.

4.2 Fracture Toughness

Fracture toughness data presented in Figure 4 clearly illustrates that the tetragonal phase is the toughening agent. When cubic ZrO_2 is incorporated into Al_2O_3, the toughness decreases. This may be a result of residual stresses associated with differential thermal expansion. Data for the series which excluded Y_2O_3 indicate that the toughness decreased with increasing monoclinic content.

Part 2 of this series presented an expression for K_c:

$$K_c = \left[K_o^2 + \frac{2(|\Delta G^c| - \Delta U_{se} f)\, E_c V_i R}{(1 - \nu_c^2)} \right]^{1/2} , \qquad (1)$$

where K_o is the critical stress intensity factor for the composite without the transformation toughening phenomena, $(|\Delta G^c| - \Delta U_{se} f)$ is the work done per unit volume to stress-induce the transformation, E_c and ν_c are the elastic properties of the composite, V_i is the volume fraction of the tetragonal ZrO_2 and R is the size of the transformation zone adjacent to the crack. By using the measured values of K_c for the series containing the tetragonal ZrO_2, the values of K_o obtained from the series containing cubic ZrO_2, E_c from Fig. 3, $\nu_c = 0.25$ and assuming that R = 1 μm (i.e., the average grain size for this series when V_i < 60 v/o ZrO_2), the average value of $(|\Delta G^c| - \Delta U_{se} f)$ was calculated as 188 MJ/m^2 for compositions containing < 60 v/o tetragonal ZrO_2. The agreement of the experimental data with this value is shown by the solid line drawn through the Al_2O_3/ZrO_2 (tetragonal) data. Although this value is in good agreement with that calculated in Part 3 for the ZrO_2 + 3 m/o Y_2O_3 material (188 MJ/m^3 vs 176 MJ/m^3), this agreement may be fortuitous since the magnitude of the terms in

($|\Delta G^c|$ - $\Delta U_{se}f$) are expected to be different for the two systems. Namely, $|\Delta G^c|$ should be greater for the ZrO_2 + 2 m/o Y_2O_3 composition relative to the ZrO_2 + 3 m/o Y_2O_3 composition, and ΔU_{se} should be greater for the higher modulus Al_2O_3/ZrO_2 constraining matrix relative to constraint with ZrO_2 alone.

As shown in Fig. 4a, good agreement between theory (Eq. 1) and data is obtained for compositions containing < 0.45 v/o ZrO_2. Poor agreement is obtained at higher volume fractions. This lack of agreement may be due to the lack of total retention of the tetragonal ZrO_2 when V_i > 60 v/o, the smaller grain size of the higher ZrO_2 compositions and/or a compositional difference due to the apparent oxygen deficiency of the ZrO_2 (see the Appendix).

4.3 Strength

The strength data presented in Fig. 5 has been analyzed to determine its dependence on the experimental K_c values. In this analysis, it was assumed that the crack size distribution responsible for failure remained unchanged from material to material. With this assumption, the strength of each material should be related by their respective critical stress intensity factors:

$$\sigma_2 = \frac{K_2}{K_1} \sigma_1 \quad . \tag{2}$$

This relation was used with the average strength and K_c for the pure Al_2O_3 to obtain the broken line in Fig. 5. As shown, three of the original five sets of data were in good agreement with this analysis, but two of the data sets (viz. V_p = 0.182 and 0.295) were higher than predicted.

Pascoe and Garvie[9] have shown that surface compressive stress arises in materials containing metastable, tetragonal ZrO_2 when the transformation at the surface is induced by an abrasion process. The volume increase associated with transformed surface layer gives rise to the compressive stresses. Since each set of strength specimens was independently surface ground, it was suspected that several of these sets (the two that resulted in the higher values) may have received surface damage to impart sufficient surface compressive stresses to increase their strength. To test this hypothesis, a small task was initiated to examine the effect of surface abrasion on strength. Although the principal results of this task will be reported elsewhere,[10] it was shown that when the abrasively ground specimens were annealed at 1300°C to eliminate the transformed surface layer, the average strength was lowered to that expected from Eq. (2). These data are shown by the open triangle in Fig. 5.

It can be concluded that the strength of the Al_2O_3/ZrO_2 (+2 m/o Y_2O_3) composite materials increases proportionally to their increase in K_c as expected. Additional strengthening can be obtained by compressive stressing the surfaces through abrasion. Studies are currently underway to characterize and optimize the abrasion phenomena.

APPENDIX:

FORMATION OF SURFACE CRACKS DURING THE HOT-PRESSING OF Al_2O_3/Al_2O_3 COMPOSITES

As indicated in the text, Al_2O_3/ZrO_2 composites containing > 30 v/o ZrO_2 hot-pressed in graphite dies were observed to contain large surface cracks. Although the exact cause of the stresses that give rise to these cracks is beyond the scope of the present work, observations do exist to indicate a probable cause.

The color of hot-pressed Al_2O_3/ZrO_2 composite billets changes from a light grey to black as the ZrO_2 volume fraction increased to 1. A color gradient also exists within a sectioned billet, darker on the outside, lighter near the center. This color gradient indicates a compositional gradient. Black ZrO_2 can also be produced at high temperatures in vacuum, and ZrO_2 is known to lose oxygen in high temperature, low oxygen environments.

XRD examination did not reveal phases other than the ZrO_2 structures indicated in the text (Table 1). Surface and interior phases were the same (precise lattice parameter measurements were not performed).

Oxidation in air at 1300°C transformed the grey to black specimens to pure white. Sectioned, oxidized specimens would reveal a dark core for short oxidation periods. Oxidation resulted in moderate to severe surface spalling for compositions containing > 30 v/o ZrO_2. The 100 v/o ZrO_2 specimens could be completely oxidized in 15 minutes at 750°C due to severe cracking.

The above evidence suggests that the dark color is consistent with an oxygen difficient ZrO_2. Ruh and Garrett[11] have shown that the oxygen difficient ZrO_2 has a smaller molar volume. Thus, a gradient in the oxygen content of the ZrO_2 from the billet surface to its interior would result in surface tensile stresses at the fabrication temperature. With a sufficient volume fraction of ZrO_2 (e.g., > 30 v/o), these tensile stresses could be significant enough to produce surface cracks. Likewise, oxidation would increase the molar volume of the depleated phase to produce surface compressive stresses and surface spalling.[12]

ACKNOWLEDGEMENTS

The careful technical services of M.G. Metcalf are deeply appreciated. The author also wishes to acknowledge the valuable discussions with D.R. Clarke and D.J. Green. Thanks are due B.R. Tittmann and E.H. Cirlin for the elastic modulus measurements. This work was supported by the Office of Naval Research under Contract N00014-77-C-0441.

REFERENCES

1. F.F. Lange, "Part 1, Size Effects Associated with Constrained Phase Transformations."

2. F.F. Lange, "Part 2, Contribution to Fracture Toughness."

3. F.F. Lange, "Part 3, Experimental Observations in the ZrO_2 - Y_2O_3 System."

4. E.M. Levin, C.R. Robbins and H.F. McMurdie, Phase Diagrams for Ceramists, 1969 Supplement, The American Ceramic Soc., 1969.

5. N. Claussen, "Fracture Toughness of Al_2O_3 with an Unstabilized ZrO_2 Dispersion Phase," J. Am. Ceram. Soc., 59, 49 (1976).

6. N. Claussen, "Stress-Induced Transformation of Tetragonal ZrO_2 Particles in Ceramic Matrices," J. Am. Ceram. Soc., 61, 85 (1978).

7. A.G. Evans and E.A. Charles, "Fracture Toughness Determinations by Indentation," J. Am. Ceram. Soc. 59, 371 (1976).

8. H.G. Scott, "Phase Relations in the Zirconia-Yittria System," J. Mat. Sci., 10, 1527 (1975).

9. R.T. Pascoe and R.C. Garvie, Ceramic Microstructures '76, ed. by R.M. Fulrath and J.A. Pask, Westview Press p. 774 (1977).

10. D.J. Green and F.F. Lange, to be published.

11. R. Ruh and H.J. Garrett, "Nonstoichiometry of ZrO_2 and its Relation to Tetragonal-Cubic Inversion in ZrO_2," J. Amer. Ceram. Soc., 50, 257 (1967).

12. F.F. Lange, "Compressive Surface Stresses Developed in Ceramics by an Oxidation-Induced Phase Change," J. Am. Ceram. Soc., 63, 38 (1980).

Table 1
FABRICATION CONDITIONS, PHASE CONTENT AND PROPERTIES OF Al_2O_3/ZrO_2 COMPOSITES

v/o ZrO_2	m/o Y_2O_3	Fabrication Condition	Density (gm/cm^3)	% ZrO_2* Phrase	H (GPa)	E (GPa)	K_c ($MPa \cdot m^{1/2}$)
		Al_2O_3/ZrO_2 (+2 m/o Y_2O_3) Series					
0	-	1400°C/2 hr	3.98	-	17.6	390	4.89
6	2	1600°C/2 hr	4.12	100t	16.8	-	5.97
12.3	2	1600°C/2 hr	4.26	100t	15.9	-	6.22
18.2	2	1600°C/2 hr	4.38	100t	16.1	356	6.58
23.9	2	1600°C/2 hr	4.50	100t	16.4	-	6.38
29.5	2	1600°C/2 hr	4.62	100t	15.7	-	7.43
45.0	2	1600°C/2 hr	4.89	trm	15.1	291	8.12
60.0	2	1600°C/2 hr	5.24	~95t	13.7	-	7.45
80.0	2	1400°C/2 hr	5.57	~85t	12.6	237	6.79
100.0	2	1400°C/2 hr	6.01	~80t	11.6	210	6.62
		Al_2O_3/ZrO_2 (pure) Series					
7.5	-	1500°C/2 hr	4.12	~90t	17.2	-	5.88
10.0	-	1500°C/2 hr	4.15	~80t	15.8	-	6.73
12.5	-	1500°C/2 hr	4.22	~70t	16.9	-	6.21
15.0	-	1500°C/2 hr	4.25	~50t	17.3	-	5.71
20.0	-	1600°C/2 hr	-	<20t	10.1	-	(5.25)
		Al_2O_3/ZrO_2 (+7.5 m/o Y_2O_3) Series					
20.0	7.5	1600°C/2 hr	4.46	100c	15.8	-	4.54
40.0	7.5	1600°C/2 hr	4.89	100c	15.9	-	3.75
60.0	7.5	1600°C/2 hr	5.28	100c	15.0	-	3.50
80.0	7.5	1600°C/2 hr	5.63	100c	14.3	-	3.14
100.0	7.5	1600°C/2 hr	5.95	100c	11.4	-	3.90

t = tetragonal
c = cubic
trm = trace monoclinic

Rockwell International
Science Center
SC5117.12TR

TRANSFORMATION TOUGHENING

PART 5: EFFECT OF TEMPERATURE AND ALLOY ON FRACTURE TOUGHNESS

F.F. Lange

Structural Ceramics Group
Rockwell International Science Center
Thousand Oaks, California 91360

ABSTRACT

The critical stress intensity facor (K_c) of materials containing tetragonal ZrO_2 was found to decrease with increasing temperature and CeO_2 alloying additions, as predicted by theory. The temperature dependence of K_c was related to the temperature dependence of the chemical free energy change associated with the tetragonal → monoclinic transformation. Good agreement with thermodynamic data available for pure ZrO_2 was obtained when the size of the transformation zone associated with the crack was equated to the size of the ZrO_2 grains. The K_c vs CeO_2 addition data was used to estimate the tetragonal, monoclinic, cubic eutectoid temperature of 270°C in the ZrO_2-CeO_2 binary system.

1.0 INTRODUCTION

In Part 2,[1] theory was presented showing that the contribution to fracture toughness (K_c) by a stress-induced transformation is proportional to the chemical free energy change ($|\Delta G^c|$) associated with the transformation. For the ZrO_2 (tetragonal) → ZrO_2 (monoclinic) transformation, $|\Delta G^c|$ is known to decrease with increasing temperature and with alloying ZrO_2 with Y_2O_3, CeO_2 etc. In this part of the series, experiments were designed to measure K_c as a function of temperature and alloy content. The temperaure dependence of K_c was measured on polycrystalline ZrO_2 and two-phase Al_2O_3/ZrO_2 materials in which 2 m/o Y_2O_3 was alloyed with the ZrO_2. The fabrication conditions and general properties of these materials have been reported in Part 4.[2]

A series of Al_2O_3/ZrO_2 materials in which CeO_2 was alloyed with the ZrO_2 phase was used to determine the effect of alloy content on K_c. As shown in Fig. 1, CeO_2 was a good candidate for this study since it forms an extensive solid-solution, tetragonal ZrO_2 phase field and lowers the tetragonal → monoclinic transformation temperature to < 25°C at ~ 20 m/o CeO_2.* Initial ZrO_2-CeO_2 sintering studies were not successful, i.e., higher CeO_2 contents (added to ZrO_2 powder as a soluable nitrate) resulted in a low density material. Hot-pressing was avoided, since CeO_2 reduces to Ce_2O_3 in environments produced by graphite dies. Attempts to sinter Al_2O_3/30 v/o ZrO_2 composite powders containing CeO_2 were successful in terms of density and phase content. Thus, these

*In contrast, the working tetragonal phase field with Y_2O_3 additions is limited to compositions between 2 and 3 m/o Y_2O_3 in both single phase tetragonal ZrO_2[3] and Al_2O_3/ZrO_2 compositions.[2]

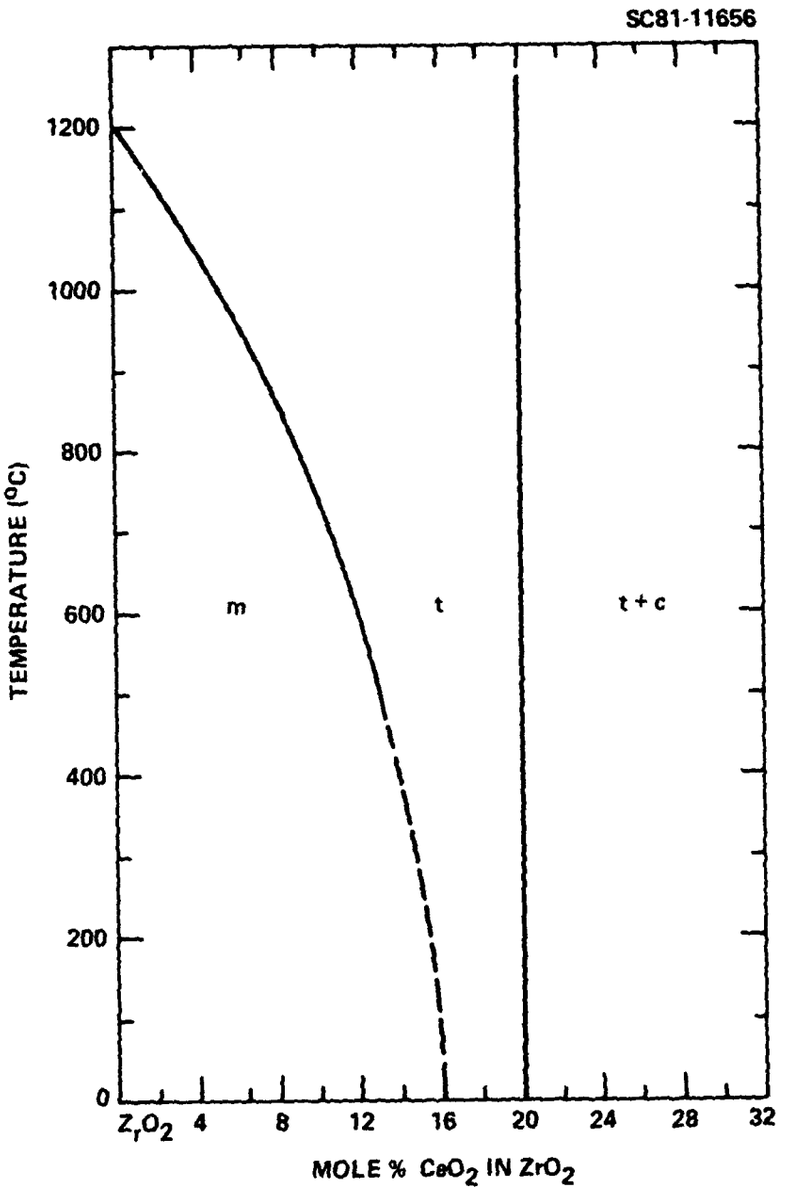

Fig. 1 A portion of the ZrO_2-CeO_2 phase diagram.[5]

composite materials were chosen for the fracture toughness vs alloying content studies.

2.0 EXPERIMENTAL

2.1 Temperature Dependence

Four materials were chosen for this study. Three of these were hot-pressed as detailed in Part 4:[2] Al_2O_3/29.5 v/o ZrO_2 (+2 m/o Y_2O_3), Al_2O_3/45 v/o ZrO_2 (+2 m/o Y_2O_3) and ZrO_2 (+2 m/o Y_2O_3). The fourth material was a Al_2O_3/30 v/o ZrO_2 (+2 m/o Y_2O_3) composite sintered to 97% of theoretical density in air at 1600°C/1 hr in which ZrO_2 was retained in its tetragonal state. The composite powders were prepared for sintering by mixing the required weight fractions of Al_2O_3,* ZrO_2** and yttrium nitrade*** by ball milling in methanol (Al_2O_3 balls and plastic bottle), drying, calcining at 500°C/4 hrs, and isostatic pressing at 350 MPa. Small bar specimens cut from each material were polished in preparation for K_c measurements.

The indentation technique, developed by Evans and Charles,[4] was used to measure K_c over the range of -196°C (liquid nitrogen) to 700°C. A Vickers diamond indentor mounted in tungsten carbide was used with the device which maintained a constant specimen temperature within the range noted. The device consisted of an internally heated copper post, mounted within a metal flask. The flask was attached to an x-y stage used to translate the specimen relative

*Lindy B, Union Carbide Corp.
**Zircar, Corp.
***Research Chemicals Corp.

to the indentor. The stage was mounted on top of a local cell and was insulated from the flask with a machinable ceramic. The specimen was spring-clip loaded in a copper well attached to the post. A chromel-alumel thermocouple, spring-clip loaded to the external face of the specimen, was used to record temperatures. For the K_c measurements at temperatures < 25°C, the flask was externally insulated and filled with liquid nitrogen. The nitrogen was allowed to slowly evaporate to achieve the desired specimen temperature. For measurements at higher temperatures, the flask was filled with insulating ceramic fiber, and the internal heater was controlled to achieve the desired temperature. Argon was forced into the metal flask to protect the copper parts and diamond from oxidation. Between measurements the indentor was held just above the specimen to avoid a large temperature differential when the indentor was again forced into the specimen at 20 Kgms. A single specimen was used for the complete temperature range investigated; two measurements were made at each temperatures.

Flexural strengh measurements were made with one of the hot-pressed materials $\left[Al_2O_3/29.5\text{ v/o }ZrO_2\text{ (+2 m/o }Y_2O_3)\right]$ over the temperature range in which K_c measurements were made. Bar specimens (0.3 × 0.6 × > 3.0 cm) were diamond cut and ground and then annealed at 1300°C for 24 hr to eliminate the surface compressive stresses developed due to the transformation of surface material during grinding.[2] Three strength measurements were made in liquid nitrogen, a mixture of dry ice and methanol, room temperature and in air at higher temperatures.

2.3 Effect of Alloying

As indicated above, a series of Al_2O_3/30 v/o ZrO_2 composite materials in which CeO_2 was incorporated were found suitable for fracture toughness vs alloying content studies. Composite powders containing the appropriate weight fractions of Al_2O_3,* ZrO_2** and CeO_2*** were mixed and milled together in plastic bottles containing methanol and Al_2O_3 mill balls, dried by flash evaporation, calcined at 500°C/16 hr, isostatically pressed into plates and sintered at 1600°C/1 hr. Sixteen compositions containing a CeO_2 content between 6 to 22 m/o CeO_2 were fabricated. Densities of these composites ranged between 94% and 98% of theoretical, based on the density of tetragonal ZrO_2 calculated using the lattice parameter of a = 5.126 A and c = 5.224 A reported by Duwez and Odell.[5] X-ray diffraction analysis of the sintered surfaces showed that 100% of the ZrO_2 was retained in its tetragonal structure for compositions containing > 12 m/o CeO_2. Trace amounts of cubic ZrO_2 were observed for compositions containing 21 and 22 m/o CeO_2, consistent with previous phase equilibria studies.[5] Increasing amounts of monoclinic ZrO_2 were observed as the CeO_2 content decreased from 11 m/o to 6 m/o. Based on these observations, composites containing > 11 m/o CeO_2 were cut and polished for fracture toughness measurements at room temperature as described above.

*Lindy B, Union Carbide Corp.
**Sub-micron ZrO_2, Zircar Corp.
***Added as Cerrium Nitrate, Research Chemicals Corp.

3.0 RESULTS

3.1 Temperature Dependence

Figure 2 illustrates that the fracture toughness decreases with increasing temperature for the four materials investigated. High, low and average values of K_c are defined by the scatter bar at each temperature. These data were fit to a linear equation:

$$K_c = A - mT \quad , \tag{1}$$

where T is temperature in degrees centigrade and the constants A and m are given in Table 1.

Table 1
Constants Defining Temperature Dependence of K_c

Material	Fabrication Conditions	A ($MPa \cdot m^{1/2}$)	m ($MPa \cdot m^{1/2}\ C^{o-1}$)	Correlation Coefficient
Al_2O_3/29.3 v/o ZrO_2 (+2 m/o Y_2O_3)	Hot-Pressed 1600°C/1 hr	7.56	0.0044	0.95
Al_2O_3/45 v/o ZrO_2 (+2 m/o Y_2O_3)	Hot-Pressed 1600°C/1 hr	6.78	0.0029	0.92
ZrO_2 (+2 m/o Y_2O_3)	Hot-Pressed 1600°C/1 hr	8.40	0.0041	0.99*
Al_2O_3/30 v/o ZrO_2 (+2 m/o Y_2O_3)	Sintered 1600°C/1 hr	9.96	0.0054	0.97

*Data at 100°C excluded.

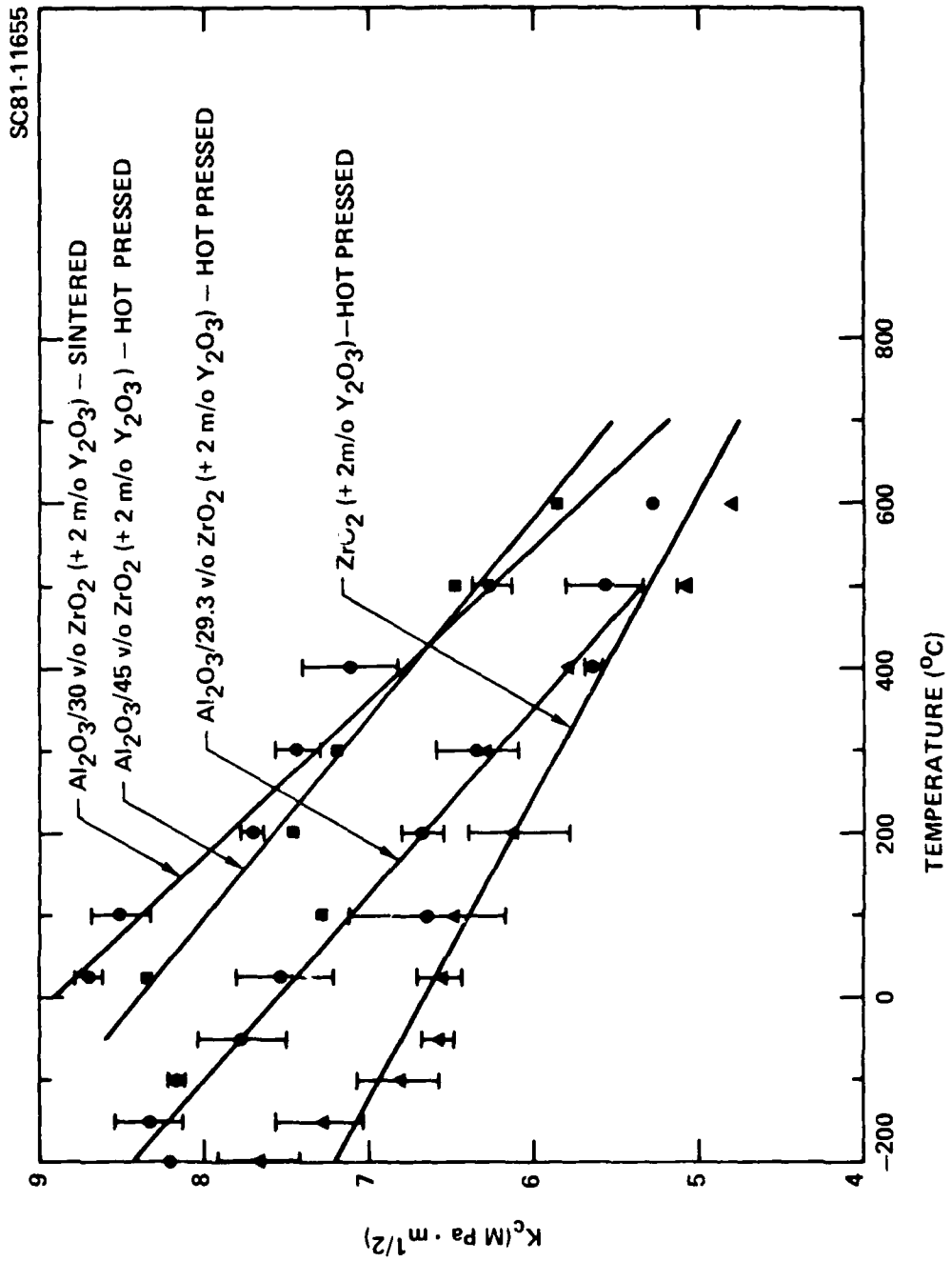

Fig. 2 Critical stress intensity factor vs temperature for the four materials investigated.

AD-A098 421 ROCKWELL INTERNATIONAL THOUSAND OAKS CA SCIENCE CENTER F/G 11/2
RESEARCH OF MICROSTRUCTURALLY DEVELOPED TOUGHENING MECHANISMS I--ETC(U)
OCT 80 F F LANGE N00014-77-C-0441
UNCLASSIFIED SC5117.8TR NL

END
DATE FILMED
5 81
DTIC

2 OF 2

AD=

AO98421

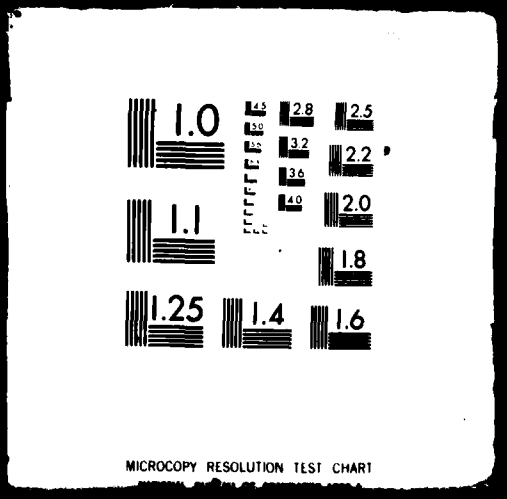

The flexural strength data for the Al_2O_3/29.3 v/o ZrO_2 (+2 m/o Y_2O_3) composites are shown in Fig. 3. These data show that strength decreases with increasing temperature. The dashed line illustrates the expected temperature behavior of strength, based on the temperature behavior of K_c as reported in Table 1 for this composition and normalizing all data to the room temperature value.

3.2 Effect of Alloying

Figure 4 reports the K_c data vs the CeO_2 addition to the ZrO_2 in the Al_2O_3/30 v/o ZrO_2 sintered materials. Data obtained for the composition containing 11 m/o CeO_2 is low due to its substantial (~ 30 %) monoclinic ZrO_2 content. Over the range where only the tetragonal ZrO_2 phase is observed (12-20 m/o CeO_2), K_c decreases with increasing CeO_2 content. K_c appears to level off to ~ 6 $MPa \cdot m^{1/2}$ at the reported tetragonal/cubic phase boundary (compositions containing > 20 m/o CeO_2). A linear relation was assumed over the range of 12-20 m/o CeO_2, resulting in the relation:

$$K_c = (10.32 - 0.202\ M)\ MPa \cdot m^{1/2} \quad , \qquad (2)$$

where M = mole% CeO_2.

4.0 DISCUSSION

In Part 2[1] of this series, it was shown that the fracture toughness of a brittle material containing a phase which would undergo a stress-induced

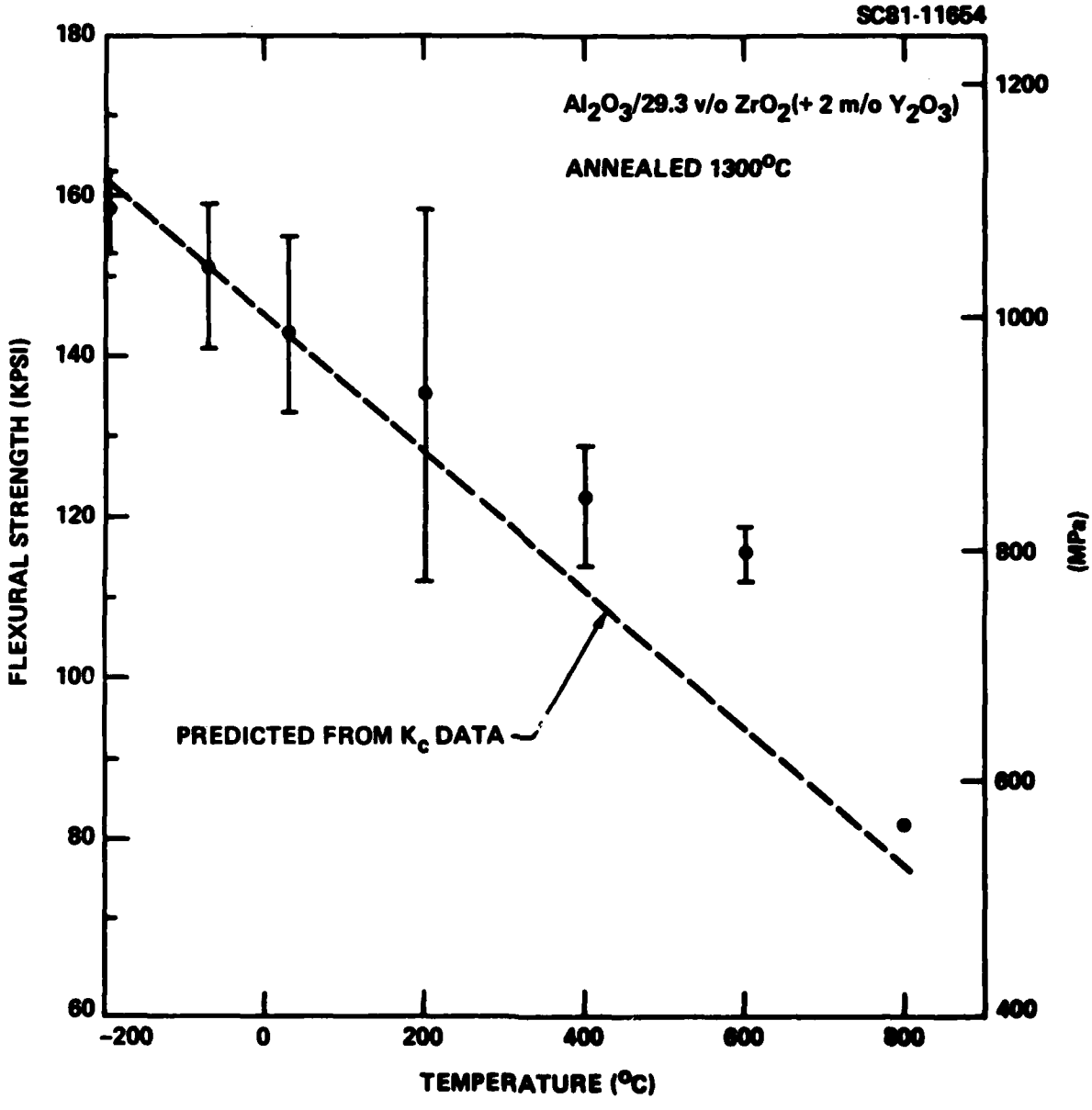

Fig. 3 Flexural strength vs temperature for the Al_2O_3/29.3 v/o ZrO_2 (+2 m/o Y_2O_3) material. Specimens first annealed at 1300°C/24 hrs.

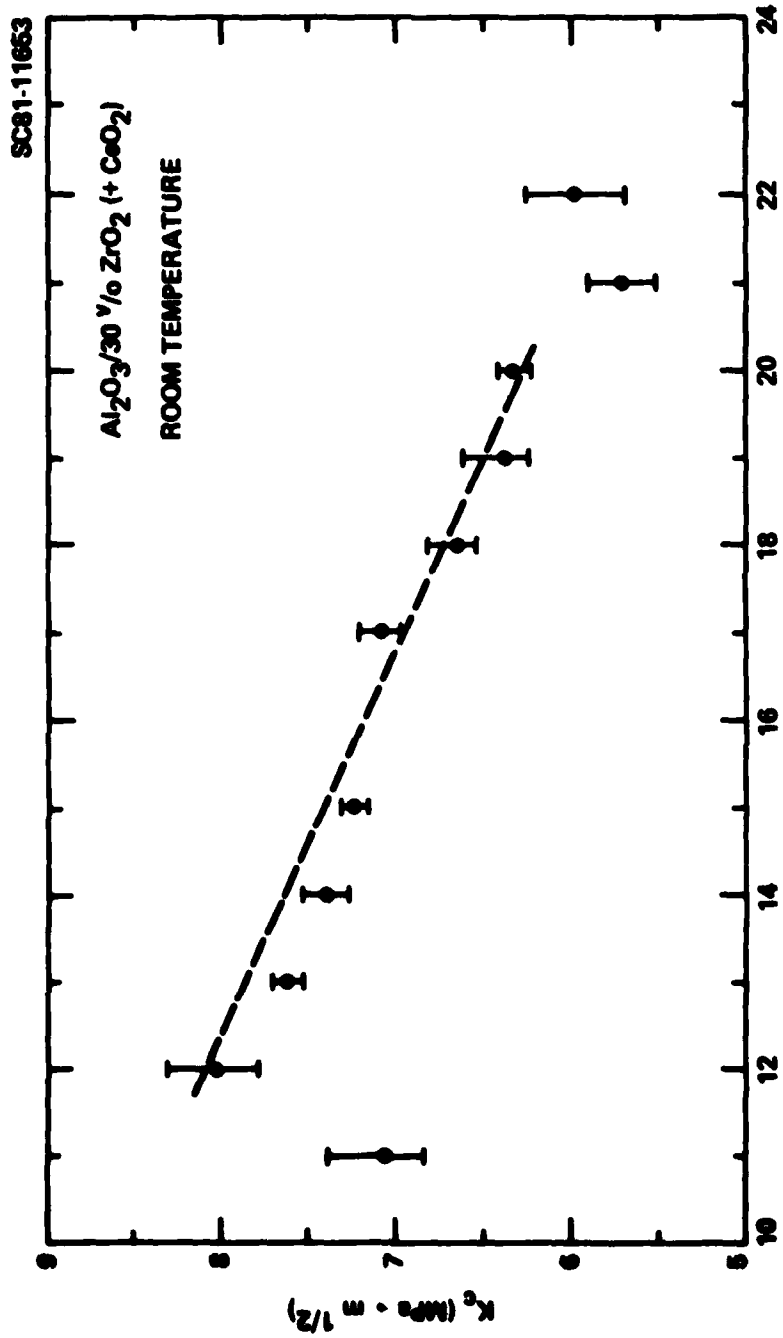

Fig. 4 Critical stress intensity factor vs mole% CeO_2 at room temperature.

transformation could be expressed as

$$K_c = \left[K_o^2 + \frac{2V_1 E_c R(|\Delta G_c| - \Delta U_{se} f)}{(1 - \nu_c^2)} \right]^{1/2}$$

where K_o is the critical stress intensity factor for the composite without the transformation toughening phenomena, E_c and ν_c are the elastic properties of the material, V_1 is the volume fraction of the phase which could undergo the stress-induced transformation, R is the size of the transformation zone adjacent to the crack and $(|\Delta G^c| - \Delta U_{se} f)$ is the work loss per unit volume during the stress-induced transformation. Since the magnitude of the chemical free-energy change associated with the transformation, $|\Delta G^c|$, is expected to exhibit the greatest dependence on temperature and alloying relative to the other factors, it was predicted that the contribution of the stress-induced transformation to fracture toughness (i.e., the second term in Eq. (3)) would have the same temperature and alloy dependence as $|\Delta G^c|$. Based on the known temperature and alloying dependence of $|\Delta G^c|$ for the $ZrO_2(t) \rightarrow ZrO_2(m)$ transformation, K_c is expected to decrease with increasing temperature and alloying content which is the general result shown in Figs. 2 and 4, respectively. The following paragraphs present more detailed analysis and discussions of these data with reference to Eq. (3).

4.1 Temperature Dependence

Based on the assumption that $|\Delta G^c|$ is the only temperature dependent factor in Eq. (3), data obtained during this study and reported in Part 4[2] were used to calculate $(|\Delta G^c| - \Delta U_{se} f)$ as a function of temperature for comparison

with the known temperature dependence of $|\Delta G^c|$ for the transformation of pure ZrO_2.[6] This calculation started by determining the size of the transformation zone, R, for each material at room temperature, using the average room temperature value of $(|\Delta G^c| - \Delta U_{se}f)$ calculated in Part 4 for a series of Al_2O_3/ZrO_2 composites, values of K_o and E_c reported* for each material in Part 4 and room temperature K_c values reported here. Table 2 lists these values and the resulting value of R as determined by rearranging Eq. (3). It should be noted that in Part 2, it was hypothosized that R ≈ the grain size; calculated values of R shown in Table 2 are consistant with the grain sizes of the ZrO_2 phase reported for the hot-pressed materials in Part 4.

In the next step, values of K_c vs temperature reported in Table 1 and the assumed temperature independent values of K_o, E_c, ν_c, V_f and R reported in Table 2 were used to calculate $(\Delta G^c - \Delta U_{se}f)$ as a function of temperature for each material by rearranging Eq. (3). These results are shown in Fig. 5;** Table 2 also reports the slope of each line $(\delta(|\Delta G^c| - \Delta U_{se}f)/\sigma T)$ and the temperature where $(|\Delta G^c| - \Delta U_{se}f) = 0$, (T_o). The fifth line drawn in Fig. 5 is the temperature dependence of $|\Delta G^c|$ for pure ZrO_2 as previously reported by Whitney.[6]

The calculations shown in Fig. 5 contain three results, which adds greater confidence to the validity of the theoretical fracture mechanics calculations (Eq. (3)). First, since $|\Delta G^c|$ is expected to exhibit the greatest temperature dependence relative to other factors in Eq. (3), the slopes of the

*As in Part 4, ν_c was assumed to be 0.25.
**The four lines coincide at 25°C since it was assumed in step one that all materials had the same value of $(|\Delta G^c| - \Delta U_{se}f)$ at 25°C.

Table 2

Values Used to Analyze K_c vs Temperature Data

Material	K_c† ($MPa \cdot m^{1/2}$)	K_o* ($MPa \cdot m^{1/2}$)	$(\Delta G^c - \Delta U_{se}f)$* ($MJ \cdot m^{-3}$)	E_c* (GPa)	ν_c*	V_f	R (μm)	$\frac{\partial(\lvert\Delta G^c\rvert - \Delta U_{se}f)}{\partial T}$ ($MJ \cdot m^{-3} + C^{\circ -1}$)	T_o (C°)
Al_2O_3/29.3 v/o ZrO_2 (+2 m/o Y_2O_3) (Hot Pressed)	7.45	4.10	188	333	0.25	0.293	0.99	-0.29	680
Al_2O_3/30 v/o ZrO_2 (+2 m/o Y_2O_3) (Sintered)	8.83	4.10	188	333	0.25	0.30	1.53	-0.27	730
Al_2O_3/45 v/o ZrO_2 (+2 m/o Y_2O_3) (Hot Pressed)	8.30	3.70	188	285	0.25	0.45	1.10	-0.21	900
ZrO_2 (+2 m/o Y_2O_3) (Hot Pressed)	6.71	3.90	188	207	0.25	1.00	0.36	-0.24	830
Average of four materials								-0.25	785
ZrO_2 (pure)[6]								-0.25	1200
$Zr_{0.96}Y_{0.04}O_{1.98}$ (ZrO_2 + 2 m/o 1/2 O_3)[7,8]									600 - 830°C

†Room temperature values, Table 1
*Room temperature values, Part 4.

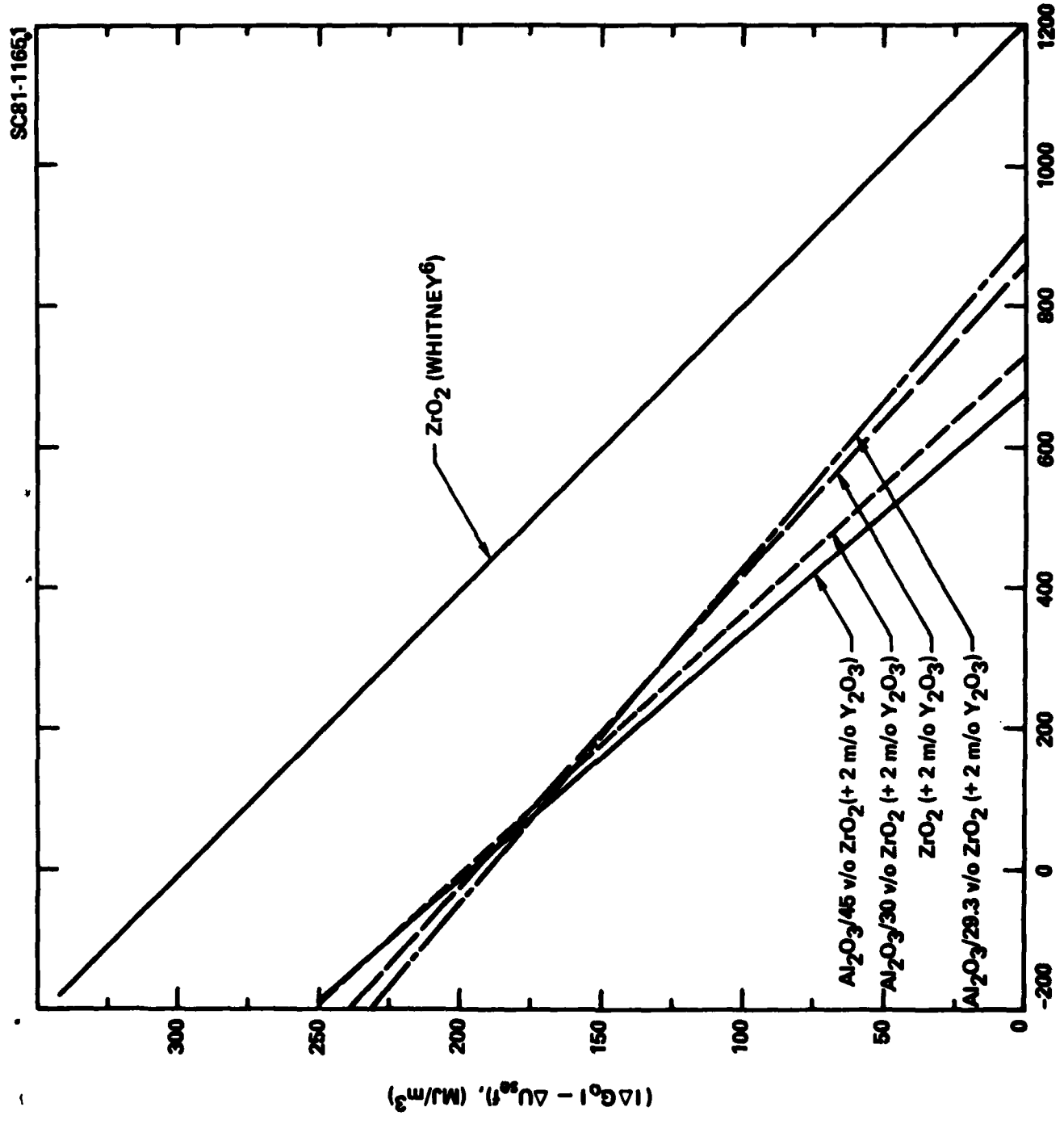

Fig. 5 Calculated values of $(|\Delta G^c| - \Delta U_{se}f)$ vs temperature for four materials studied. Upper line is $|\Delta G^c|$ vs temperature for pure ZrO_2 as

four lines in Fig. 5 should be the same as $\delta|\Delta G^c|/\delta T$ for $Zr_{0.96}Y_{0.04}O_{1.98}$ (ZrO_2 + 2 m/o Y_2O_3). Although $|\Delta G^c|$ vs temperature data do not exist for this solid-solution compound, it is important to note that the slopes are nearly coincident (see Table 2) for that of pure ZrO_2 as reported by Whitney.[6] Second, the temperature (T_o) where ($|\Delta G^c| - \Delta U_{se}f$) = 0 lie within the range of transformation temperatures (where $\Delta G^c = 0$) (see Table 2) for $Zr_{0.96}Y_{0.04}O_{1.98}$ powder.[7,8] This result suggests that the residual strain energy associated with the ZrO_2 grains that contribute most to the fracture toughness is very small, viz. $\Delta U_{se}f \approx 0$. Third, the slope of the lines in Fig. 5 critically depend on the value of R chosen, i.e., larger or smaller values of R would not have resulted in the good agreement with $\delta|\Delta G^c|/\delta T$ for pure ZrO_2. Values of R calculated from room temperature data* (Step 1) not only result in reasonable slopes for $\delta|\Delta G^c|/\delta T$, but they are also in good agreement with the size of the ZrO_2 grains as hypothesized by theory.

4.2 Effect of Alloying

Based on the assumption that $|\Delta G^c|$ is the only factor in Eq. (3) affected by alloying CeO_2 with ZrO_2, the K_c results presented in Eq. (2) have been used to calculate the combined factor ($|\Delta G^c| - \Delta U_{se}f$)R. The linear expression resulting from combining Eq. (2) and (3) with the appropriate values[2]

*A second approach can also be used to determine R for each material by calculating the combined product R($|\Delta G^c| - \Delta U_{se}f$) in Eq. (3) as a function of temperature and assuming that $\delta(|\Delta G^c| - \Delta U_{se}f)/\delta T = 0.248$ $MJ \cdot m^{-3} \cdot C^{\circ -1}$ (the value of $\delta|G_c|/\delta T$ for pure ZrO_2).[6] Using this approach, values of R for the four materials listed in Table 2 are 1.2 μm, 1.65 μm, 0.95 μm and 0.34 μm, respectively.

K_o = 4.1 MPa $m^{1/2}$, E_o = 333 GPa, ν_c = 0.25 and V_f = 0.30 for the Al_2O_3/30 v/o ZrO_2 (+ CeO_2) compositions is

$$(|\Delta G^c| - \Delta U_{se}f)R = (415 - 15.8\ M)\ MJ/m^2 \quad . \quad . \quad (4)$$

Equation (4) can be used to estimate two thermodynamic properties of ZrO_2, which again adds greater confidence to the fracture mechanisms theory as expressed in Eq. (3). First, by extrapolating the data obtained between M = 12 to 20 m/o CeO_2 to M = 0, one obtains the value of $(|\Delta G^c| - \Delta U_{se}f)R$ = 415 MJ/m^2 for pure ZrO_2. By chosing R = 1.5 μm, the value determined to be consistent with the K_c vs temperature data for a similar, sintered Al_2O_3/30 v/o ZrO_2 composite discussed in the last section, one obtains $(|\Delta G^c| - \Delta U_{se}f)$ = 275 MJ/m^3. It is interesting to note that this value agrees almost exactly with the room temperature value of $|\Delta G^c|$ = 290 MJ/m^3 for pure ZrO_2 as previously calculated by Whitney (see Fig. 5). Although this near perfect agreement may be fortuitous, it again suggests that the residual strain energy ($\Delta U_{se}f$) associated with the transformed grains adjacent to the crack surfaces can be neglected in estimating their contribution to fracture toughness.

Second, previous phase equilibria work[5] in the ZrO_2-CeO_2 binary system has suggested that CeO_2 additions in the range between 15 to 20 m/o CeO_2 lowers the tetragonal → monoclinic transformation temperature below 25°C. K_c measurements (see Fig. 2) clearly show that the tetragonal phase contributes to toughening over the complete range of CeO_2 studied (11 m/o to 22 m/o). That is, K_c measurements strongly suggest that the eutectoid temperature is > 25°C. Using the fracture mechanics data, one can estimate the eutectoid temperature by

assuming that $\Delta U_{se}f = 0$ and determing the value of M in Eq. (4) where $|\Delta G^c|R = 0$. This condition exists when M = 26 m/o CeO_2. By constructing a line between 1200°C and 26 m/o CeO_2 on the ZrO_2-CeO_2 phase diagram and recognizing that the tetragonal + cubic phase field exists when M > 20 m/o CeO_2, one estimates the eutectoid temperature as 270°C which alters the phase diagram shown in Fig. 1 to that shown in Fig. 6.

5.0 CONCLUSIONS

1. The fracture toughness of materials containing tetragonal ZrO_2 decreased with increasing temperature and alloying addition, consistent with theoretical predictions.

2. An analysis of the data suggests that the residual strain energy associated with the transformed ZrO_2 gains can be neglected. Thus, the equation which appears to explain the contribution of the stress-induced phase transformation to fracture toughness can be rewritten as

$$K_c = \left[K_o^2 + \frac{2|\Delta G_c|E_c V_f R}{(1 - \nu_c^2)}\right]^{1/2} . \qquad (5)$$

3. The fracture mechanics data, when analyzed with respect to theory as expressed by Eq. (3), best fit the thermodynamic data for ZrO_2 when it was assumed that the size of the transformation zone is the same size as the ZrO_2 grains.

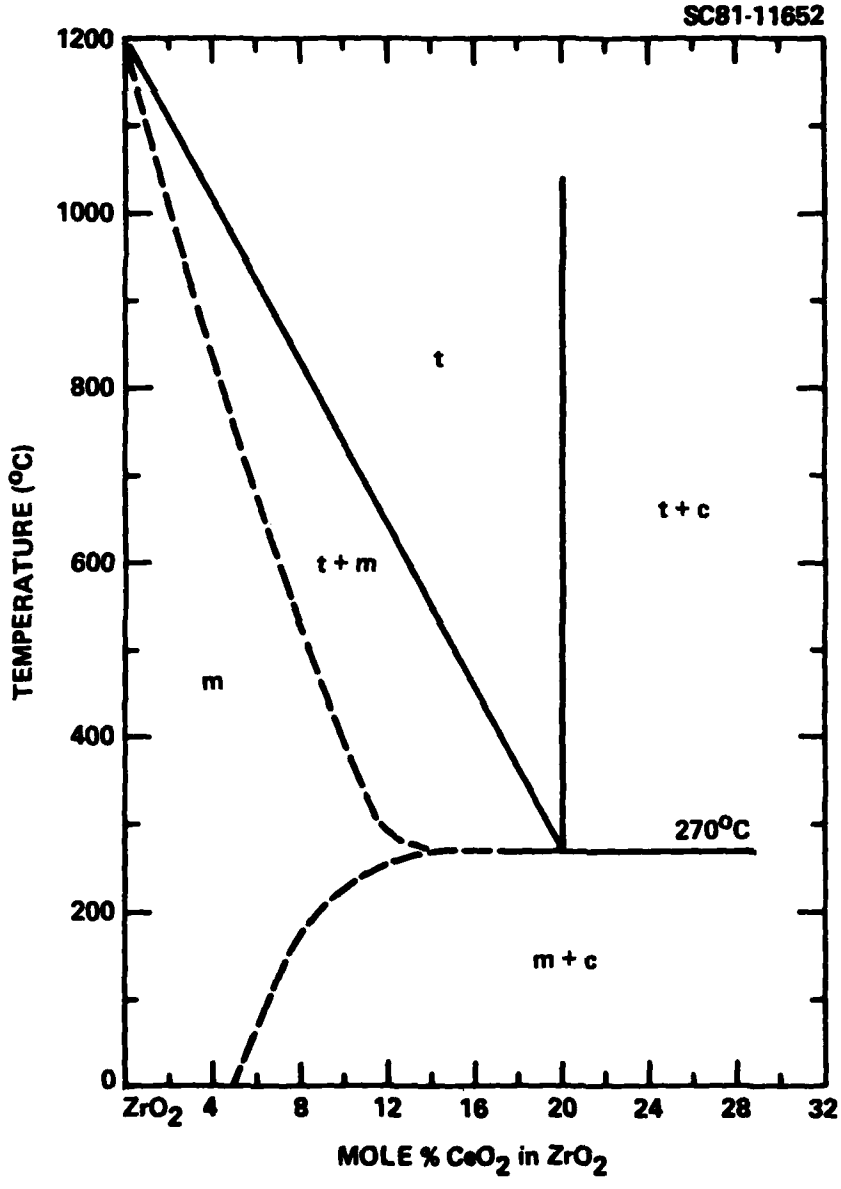

Fig. 6 A portion of the ZrO_2-CeO_2 phase diagram, in which the eutectoid temperature has been estimated through fracture mechanics data.

ACKNOWLEDGMENTS

The technical assistance of Milan Metcalf was greatly appreciated. This work was supported by the Office of Naval Research under Contract N00014-77-C-0441.

REFERENCES

1. F.F. Lange, "Part 2, Contribution to Fracture Toughness."
2. F.F. Lange, "Part 4, Fabrication, Fracture Toughness and Strength of Al_2O_3/ZrO_2 Composites."
3. F.F. Lange, "Part 3, Experimental Observations in the ZrO_2-Y_2O_3 System."
4. A.G. Evans and E.A. Charles, "Fracture Toughness Determination by Indentation," J. Am. Ceram. Soc. 59 (7-8), 371 (1976).
5. P. Duwez and F. Odell, "Phase Relationships in the System Zirconia-Ceria," J. Am. Ceram. Soc. 33, [9], 274 (1950).
6. E.D. Whitney, "Effect of Pressure on Monoclinic-Tetragonal Transition of Zirconia; Thermodynamics," J. Am. Ceram. Soc. 45 [12], 612 (1962).
7. K.K. Svirastoka, R.N. Patil, C.B. Chandry, K.V.G.K. Gokhale and E.C. Subbaro, "Revised Phase Diagram of the System ZrO_2-Y_2O_3," Trans. Brit. Ceram. Soc. 73, 85 (1974).
8. H.G. Scott, "Phase Relations in the Zirconia-Yttria System," J. Mat. Sci. 10, 1527 (1975).


DAT
FILM